HHS Public Access

Author manuscript

Cell Rep. Author manuscript; available in PMC 2023 October 31.

Published in final edited form as:

Cell Rep. 2023 September 26; 42(9): 113057. doi:10.1016/j.celrep.2023.113057.

Cerebellar interneurons control fear memory consolidation via learning-induced HCN plasticity

Kathryn Lynn Carzoli[1,2,3], **Georgios Kogias**[1,2,3], **Jessica Fawcett-Patel**[1,2], **Siqiong June Liu**[1,2,4,*]

[1]Department of Cell Biology and Anatomy, Louisiana State University Health Sciences Center, New Orleans, LA 70112, USA

[2]Southeast Louisiana VA Healthcare System, New Orleans, LA 70119, USA

[3]These authors contributed equally

[4]Lead contact

SUMMARY

While synaptic plasticity is considered the basis of learning and memory, modifications of the intrinsic excitability of neurons can amplify the output of neuronal circuits and consequently change behavior. However, the mechanisms that underlie learning-induced changes in intrinsic excitability during memory formation are poorly understood. In the cerebellum, we find that silencing molecular layer interneurons completely abolishes fear memory, revealing their critical role in memory consolidation. The fear conditioning paradigm produces a lasting reduction in hyperpolarization-activated cyclic nucleotide-gated (HCN) channels in these interneurons. This change increases intrinsic membrane excitability and enhances the response to synaptic stimuli. HCN loss is driven by a decrease in endocannabinoid levels via altered cGMP signaling. In contrast, an increase in release of cerebellar endocannabinoids during memory consolidation abolishes HCN plasticity. Thus, activity in cerebellar interneurons drives fear memory formation via a learning-specific increase in intrinsic excitability, and this process requires the loss of endocannabinoid-HCN signaling.

Graphical abstract

*Correspondence: sliu@lsuhsc.edu.

AUTHOR CONTRIBUTIONS

K.L.C. and S.J.L. were responsible for the concept and design of the study. K.L.C., G.K., and J.F-P. performed the experiments, analyzed data, and made figures. K.L.C., G.K., and J.F.-P. were involved in the design and refinement of the methodological procedures and participated in interpreting the findings. K.L.C., G.K., and S.J.L. drafted the manuscript. All authors critically reviewed and approved the final version for publication.

SUPPLEMENTAL INFORMATION

Supplemental information can be found online at https://doi.org/10.1016/j.celrep.2023.113057.

DECLARATION OF INTERESTS

The authors declare no competing financial interests.

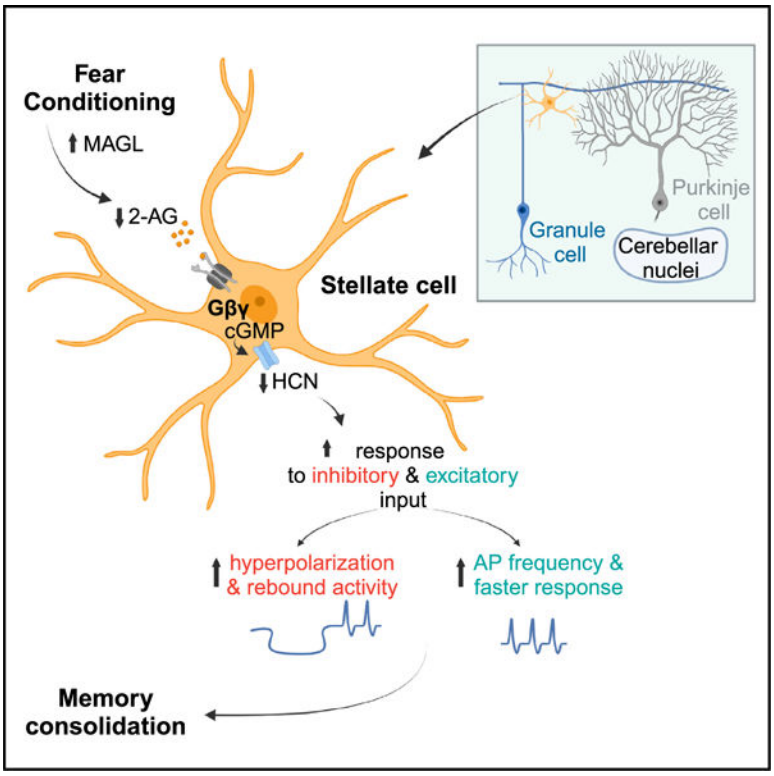

In brief

Carzoli et al. reveal that activity in cerebellar interneurons drives fear memory formation via a learning-specific increase in intrinsic excitability, and this process requires the loss of endocannabinoid-HCN signaling. This highlights the importance of moving beyond traditional synaptic plasticity-focused investigations of memory formation.

INTRODUCTION

While bidirectional modifications in synaptic efficacy underlie multiple forms of learning and memory, the intrinsic excitability of a neuron assimilates and translates synaptic input into a particular output. Learning-induced changes in intrinsic membrane properties can alter neuronal circuit activity and resulting behavior, highlighting the importance of moving beyond traditional synaptic plasticity-focused investigations of memory formation. Thus, there is a need to understand the mechanisms underlying learning-induced changes in intrinsic excitability in neurons that encode memory formation, as well as to identify the ion channels driving variation in neuronal excitability.[1,2] The hyperpolarization-activated cyclic nucleotide-gated (HCN) channel determines neuronal active and passive membrane properties,[3] and deletion of the HCN gene impairs cerebellum-dependent motor learning but improves hippocampus-dependent spatial learning.[4–6] We therefore hypothesized that a learning-induced change in the nonselective cation current that is carried by HCN (I_h) would alter neuronal intrinsic excitability and ultimately govern cerebellar-dependent memory formation.

Associative emotional learning involves multiple brain regions, including the cerebellum, where the underlying mechanisms are not known. In particular, the cerebellum plays an important role in the consolidation of Pavlovian fear-conditioned (FC) memories, as inactivation or lesion of the vermis after memory acquisition disrupts conditioned defense responses in animals and humans.[7–9] Given the extensive reciprocal connections that exist between the cerebellum and cortical and subcortical regions, one fundamental question is whether the cerebellar circuit acts as a relay station or actively participates in encoding memory formation processes. Our recent study showed that FC reduces endocannabinoid (eCB) signaling in the cerebellar cortex and that this change is required for memory consolidation,[10] demonstrating a critical role of cerebellar circuit plasticity in learned fear. FC produces long-term potentiation at both excitatory and inhibitory synapses onto Purkinje cells (PCs)[11,12] and enhances feedforward inhibitory connectivity[13] but does not alter PC excitability.[14] Given that inhibitory interneurons innervate PCs and thus control the output of the cerebellar cortex, a learning-induced change in interneuron activity would be a strong candidate for driving memory consolidation.

Here, we found that silencing molecular layer interneurons (MLIs) with Gi-coupled designer receptors exclusively activated by designer drugs (Gi-DREADD) abolished memory consolidation, demonstrating that cerebellar MLI activity drives memory formation. We determined the impact of learning on I_h and intrinsic membrane properties and found that FC reduced I_h in cerebellar stellate cells (SCs). This increased membrane excitability and consequently enhanced the response of SCs to both depolarizing and hyperpolarizing inputs. Mechanistically, this involved a learning-induced decrease in eCB signaling producing loss of HCN via regulation of cyclic guanosine monophosphate (cGMP). Importantly, disrupting memory formation, by elevating eCBs in the cerebellum *in vivo*, impaired HCN plasticity. These results demonstrate a form of plasticity, in which a learning-induced depletion of eCBs disrupts interneuron HCN function and drives memory formation in the cerebellum.

RESULTS

Molecular layer interneuron activity is required for memory consolidation

Fear conditioning enhances GABA release from MLIs that control the activity of PCs. We tested the hypothesis that cerebellar MLI activity is required for fear memory consolidation by injecting viral Gi-DREADD$^{f/f}$ vector into vermal lobules V/VI in nitric oxide synthase (NOS)-cre mice (NOS::Gi) to selectively silence MLIs, the only cerebellar neurons that express NOS. Two weeks later, we observed mCherry-expressing cells located solely in the molecular layer that displayed spontaneous action potential firing, an MLI characteristic. We then confirmed that application of CNO (clozapine N-oxide), a synthetic ligand for DREADD receptors, activated Gi-DREADD receptors on MLIs and suppressed spiking activity and that spontaneous activity recovered on CNO removal (Figures 1A and 1B).

NOS::Gi mice were subjected to an FC protocol, in which they were presented with a tone (conditioned stimulus) followed by a temporally contiguous foot shock (unconditioned stimulus) and received CNO or saline injection 30 min later, during the consolidation period. Both groups exhibited freezing response during the last three tones (CNO: 43% ± 8% and saline: 37% ± 6%; Tukey's post hoc: $p = 0.81$). The following day, mice were

exposed to tone alone in a new context to test their cued memory retention. We found that mice administered with CNO showed no freezing responses to tone, whereas those that received saline exhibited ~50% freezing (two-way repeated measures [RM] ANOVA: $F_{4,30} = 7.43$, $p < 0.0005$; Bonferroni post hoc: $p = 0.0003$; Figures 1C and 1D). We next administered CNO to NOS:mCherry mice to test for any off-target effects of the drug and its metabolites on memory formation. These mice responded to tone during learning as NOS::Gi animals (Bonferroni post hoc: $p = 1$). The freezing behavior of FC mice during the memory retention test was comparable to saline-injected animals and markedly greater than NOS::Gi mice receiving CNO (Bonferroni post hoc: $p = 0.017$). Therefore, silencing MLIs through activation of Gi-DREADD abolished memory consolidation. When viral injection missed vermal lobules V/VI, the defensive response during memory retention (46% ± 8%, $n = 3$) was not different from NOS:mCherry control mice (unpaired t test: $p = 0.82$). These results demonstrate that MLI activity in vermal lobules V/VI drives the formation of fear memory.

Associative FC induces a lasting decrease in cerebellar interneuron I_h

Hyperpolarization-activated cation channels are present in MLIs and can be modulated by cAMP via activation of β-adrenergic receptors.[15] Since neural plasticity is thought to be a cellular substrate of learning and memory, we characterized HCN channel properties in cerebellar SCs of vermal lobules V/VI, where sensory inputs carrying information about the conditioned and unconditioned stimuli converge.[16,17] A series of hyperpolarizing stimuli delivered to SCs elicited both instantaneous and late, inward currents. Subtraction of the instantaneous component from the total current revealed a voltage-dependent, slowly activating, inward current of −69 ± 7 pA at −120 mV. Bath application of the HCN channel blockers ZD7288 and CsCl caused a large reduction in I_h (86% and 78%, respectively). A comparison of drug-sensitive and slow-activating currents revealed similar amplitudes (Figure S2), confirming their mediation by HCN channels. The activation time constant of I_h, ~70 ms (Figure S3), is comparable with the more rapid kinetics of recombinant HCN1 channels[18] and is consistent with the expression of HCN1 and HCN4 mRNA in molecular layer neurons (Allen Brain Atlas).

To determine the effect of FC on stellate cell HCN, mice were subjected to a fear conditioning protocol, and cerebellar slices were prepared 24 h later (Figures 1E, 1F, and S3A). Whole-cell voltage clamp revealed a large attenuation in mean I_h amplitude, from −80 ± 12 pA in naive mice to −19 ± 2 pA after FC, in response to a −120-mV step (unpaired t test: $t_{11} = 5.5$, $p < 0.001$; Figures 1G and 1H). I_h activation kinetics did not differ between groups (two-way RM ANOVA: $F_{2,32} = 1.3$, $p = 0.3$; Figure S3C), suggesting HCN subunit composition was unlikely altered by FC. When mice were exposed to tones and shocks in an unpaired manner, average steady-state amplitudes were similar to the naive group (−63 ± 6 pA, unpaired t test: $t_{10} = 1.2$, $p = 0.25$) but reduced by 70% after FC (two-way RM ANOVA: behavior, $F_{1,8} = 44.8$, $p < 0.001$; Figures 1F–1H). Since slowly activating and ZD7288 (or CsCl)-sensitive current amplitudes in both naive and unpaired animals were greater than those recorded after FC (two-way ANOVA, behavior, $I_{ZD\text{-}sensitive}$: $F_{2,40} = 43.7$, $p < 0.00001$; $I_{CsCl\text{-}sensitive}$: $F_{1.26} = 28.68$, $p < 0.0001$; Figure S3B), our findings indicate that I_h loss is caused by a learned tone-shock association.

We evaluated spatial characteristics of the FC-induced change in HCN since synaptic plasticity is lobule specific.[10,11] In naive mice, I_h amplitude in lobule IX—a lobule involved in motor coordination—was comparable to the current recorded in lobules V/VI (unpaired t test: $t_{10} = 1.3$, $p = 0.2$). In contrast to lobules V/VI, recordings made in lobule IX of conditioned mice revealed no reduction in I_h amplitude relative to naive animals (two-way RM ANOVA: $F_{1,56} = 1.1$, $p = 0.3$; Figures 1I, 1J, and S3D). These results highlight the spatially selective nature of the FC-induced change in HCN (FC: $I_h^{V/VI}$ vs. I_h^{IX}, unpaired t test: $t_{10} = -14.1$, $p < 0.001$).

We next characterized temporal features of the fear conditioning-induced change in HCN current (Figure S4A), as cerebellar activity is required for cued fear memory formation up to 8 days after acquisition.[8] When cerebellar slices were prepared 3 h after fear conditioning, the amplitude of slow-activating inward HCN current (−57 ± 2 pA, n = 5) was indistinguishable from naive control (−68 ± 5 pA, n = 11) but greater than the current recorded at 24 h post learning (one-way ANOVA: $F_{3,25} = 31.9$, $p < 0.0001$; Tukey's post hoc, naive vs. 3 hr post FC, $p = 0.29$; 3 h vs. 24 h post FC, $p = 0.00009$; Figures 2A–2E), indicating the significant decrease in I_h occurred between 3 and 24 h. To determine whether the FC-induced decrease in HCN current is a long-lasting change, we quantified I_h in SCs 7 days after fear conditioning. The amplitude of I_h remained at −25 ± 2 pA (n = 6), comparable to the HCN current recorded 1 day after learning but markedly lower than naive control (Tukey's post hoc, 1 day vs. 7 days post FC: $p = 0.44$; naive vs. 7 days post FC: $p < 0.000001$, Figures 2A–2C). Therefore, fear conditioning produced a sustained decrease in HCN current that lasted for at least 7 days.

Learning-induced decrease in endocannabinoid signaling suppresses I_h

We recently reported a decrease in the level of 2-arachidonoylglycerol, an eCB, in cerebellar lobules V/VI following FC, which lasts for at least 24 h, and that this reduction is responsible for memory consolidation.[10] The decrease in 2-AG levels did not alter the function of CB1Rs, as the CB1R agonist was able to suppress mIPSC frequency in MLIs from conditioned animals to the same extent as in controls. Since CB1R activation can increase I_h in a subset of hippocampal CA1 pyramidal neurons,[19] we hypothesized that the learning-induced decrease in eCB signaling is what drives the loss of I_h in cerebellar SCs. We asked whether eCB signaling regulates I_h in SCs from naive mice and found that application of a CB1R neutral antagonist, NESS0327, caused a 50% decrease in I_h amplitude at −120 mV (Holm-Sidak post hoc: $t_{13} = 5.9$, $p < 0.001$; Figures 2D, 2E, and 2L). HCN conductance increased as the membrane potential became more hyperpolarized. Calculating V_{50}, the potential that gives half of the maximal conductance, revealed a hyperpolarizing shift on CB1R antagonist application from −72 mV to −83 mV (Holm-Sidak post hoc: $t_{13} = -2.6$, $p = 0.017$; Figures 2H and 2I). Conversely, application of the CB1R agonist, WIN55,212–2, increased I_h amplitude and shifted activation to −63 mV (Holm-Sidak post hoc, amplitude: $t_{12} = -3.3$, $p = 0.0038$; V_{50}: $t_{12} = 2.2$, $p = 0.044$; Figures 2F–2I). These findings suggest that CB1R regulates I_h amplitude and activation in SCs and that tonic eCB is the primary modulator that sets basal I_h.

We next determined the effect of the learning-induced decrease in eCB on I_h. HCN conductance showed a more hyperpolarized activation voltage in SCs from conditioned mice (V_{50} = −83 ± 2.6 mV) compared to naive controls (unpaired t test: t_{17} = 3.3, p = 0.0057; Figures 2J–2L). The learning-induced hyperpolarizing shift persisted for 7 days, relative to HCN activation 3 h after acquisition that was comparable to naive controls (Figures S4B and S4C). NESS0327 application did not further reduce I_h amplitude nor shift its activation (Figures 3A–3C, 3J, and 3K), suggesting that a learning-induced decrease in eCB occluded the effects of NESS0327 on HCN in controls. CB1R activation with WIN55,212–2 increased the amplitude of I_h to −65 ± 7pA and caused a depolarizing shift in activation (V_{50} −70 ± 2 mV) that was comparable to controls (vs. no WIN, Holm-Sidak post hoc, amplitude: t_{14} = −7.4, p < 0.0001; V_{50}: t_{14} = 3.1, p = 0.005; Figures 3D–3F, 3J, and 3K). Elevating levels of the endogenous eCB, 2-arachidonoylglycerol (2-AG), by inhibiting monoacylglycerol lipase (MAGL) with JZL184 restored both I_h amplitude (−72 ± 7 pA) and activation voltage (−71.6 ± 1 mV) to naive levels (Holm-Sidak post hoc, amplitude: t_{14} = −8.6, p < 0.0001; V_{50}: t_{14} = −2.6, p < 0.015; Figures 3G–3K). Current amplitude also exhibited a strong correlation with the half-maximal activation voltage (R^2 = 0.92; Figure 4L). These results indicate that a learning-induced disruption in eCB signaling reduces HCN activation at physiological potentials and diminishes I_h.

We predicted that increasing eCB signaling in the cerebellum *in vivo* would prevent I_h plasticity and disrupt memory consolidation. Our recent study showed that chemogenetic stimulation of Gq-DREADD in PCs triggers eCB release and, importantly, that eCB signaling impairs memory consolidation.[10] To test our hypothesis that this would block the learning-induced decrease in SC I_h, we took advantage of the selective expression of L7 protein in PCs[20] by crossing GqDREADD and L7-cre lines. Both L7:Gq(+) and L7:Gq(−) mice were subjected to FC and received a CNO injection 30 min later (Figures 4A and 4B). In SCs from L7:Gq(−) mice, both I_h amplitude (−21 ± 3 pA) and activation voltage (V_{50} = −89 ± 3 mV) were indistinguishable from conditioned wild-type mice (unpaired t test, I_h: p = 0.18; V_{50}: p = 0.21). CB1R antagonism with NESS0327 failed to reduce I_h magnitude or modify activation voltage (unpaired t test: p > 0.15, Figures 4C–4E), indicating that learning reduced eCB signaling. Recordings made in SCs from conditioned L7:Gq(+) animals revealed a 3-fold greater current amplitude at −120 mV than that in L7:Gq(−) mice (unpaired t test: p < 0.0001; Figures 4F, 4G, and 4I). HCN conductance showed a depolarizing shift relative to L7:Gq(−), with a V_{50} of −69 ± 3 mV (unpaired t test: p < 0.0002; Figures 4H and 4J). This difference was lost when NESS0327 was applied, as the current amplitude in L7:Gq(+) animals decreased by 56% (Holm-Sidak post hoc: t_{10} = 7.72, p < 0.0001; Figures 4F–4J) while the activation curve shifted toward a more hyperpolarized potential (V_{50} = −85 ± 2 mV; Holm-Sidak post hoc: t_{10} = −3.8, p < 0.001; Figures 4H and 4J). Both I_h amplitude and half-activation voltage in L7:Gq(+) mice were comparable to naive controls. Therefore, stimulation of Gq-DREADD in PCs prevented the learning-induced loss of I_h in MLIs by increasing eCB signaling. These results reveal that cerebellar MLI activity is required for memory consolidation, where HCN plasticity driven by a depletion of eCB signaling enhances SC intrinsic excitability and promotes memory formation.

Endocannabinoid signaling elevates I_h via $G_{\beta\gamma}$-JNK-NOS-cGMP

HCN channels are gated by cyclic adenosine monophosphate (cAMP) and cGMP. CB1R agonists can increase I_h by elevating cGMP through activation of G protein $\beta\gamma$ subunits ($G_{\beta\gamma}$) and c-JUN-N-terminal-kinases (JNKs).[19] The latter stimulates NOS and the NO-sensitive guanylyl cyclase (GC). We therefore tested whether eCB signaling in cerebellar SCs regulates I_h via a cGMP-dependent pathway.

Selective interference of $G_{\beta\gamma}$-cGMP signaling by inclusion of either $G_{\beta\gamma}$ or JNK inhibitors in the recording pipette revealed that both components are required for the CB1R-dependent increase in SC I_h in conditioned mice. The presence of the $G_{\beta\gamma}$ inhibitor, gallein, had no effect on basal I_h amplitude or activation, consistent with a lack of tonic eCB signaling after FC. CB1R agonism with WIN55,212–2 failed to increase the current amplitude or cause a depolarizing shift in I_h activation (Figures 5A–5C, 5P, and 5Q). The JNK inhibitor, SP600125, also prevented the increase in current amplitude and depolarizing shift in activation seen on WIN application without affecting basal I_h (Figures 5D–5F, 5P, and 5Q).

We next tested whether the CB1R-Gβγ-JNK pathway increases cGMP production to elevate I_h. Blocking GC with ODQ did not alter basal I_h but completely abolished the WIN55,212–2-induced increase in I_h amplitude and depolarizing shift in activation (Figures 5G–5I, 5P, and 5Q). We further examined whether NOS was necessary since GC is sensitive to NO levels. Intracellular application of the NOS inhibitor, L-NAME, eliminated the WIN55,212–2-induced increase in I_h amplitude and depolarizing shift in activation but had no effect on basal current (Figures 5J–5L, 5P, and 5Q). Like cGMP, cAMP has the potential to enhance HCN; however, inclusion of an adenylyl cyclase inhibitor in the pipette solution failed to block the increased amplitude and depolarizing shift in activation seen with WIN55,212–2 (Holm-Sidak post hoc, I_h amplitude: $t_9 = -8.0$, $p < 0.0001$; V_{50}: $t_9 = 3.5$, $p < 0.0001$; Figures 5M–5Q). Therefore, in control conditions, the CB1R-$G_{\beta\gamma}$-JNK pathway promotes cGMP production via NOS-GC, enabling I_h activation at resting potentials and increasing current amplitude. A 10- to 15-mV shift in I_h activation suggests that HCN channels in MLIs include cGMP-sensitive HCN4 subunits[21] and most likely are formed by HCN1 and 4 subunits.

Reduction of I_h augments the SC response to hyperpolarizing input

Our recordings of SCs from naive and FC animals at 34°C–37°C showed an insensitivity of I_h amplitude and voltage dependence to temperature but faster activation kinetics at 37°C (Figures S4D–S4F). As such, all current-clamp and cell-attached recordings were performed at near physiological temperature. In naive animals, injection of a negative current step (−75 pA) produced a rapid hyperpolarization followed by a depolarizing inflection that was completely blocked by ZD7288. This ‘‘voltage sag’’ was reduced by 58% in FC animals (Figures 6A and 6B), and application of ZD7288 further blocked the remaining sag response indicating a large reduction of functional HCN in cerebellar SCs after learning.

Because I_h typically reverses around −40 mV, HCN channels generate an excitatory inward current at subthreshold potentials, contributing to both a cell’s resting conductance and

active membrane properties.[3] We assessed the effect of learning on SC input resistance (R_{in}), which is crucial in determining a neuron's voltage response to current, and we found that FC markedly increased stellate cell R_{in} (798 ± 78 MΩ) relative to naive conditions (452 ± 42 MΩ; two-way RM ANOVA: $F_{1,13} = 8.06$, $p = 0.014$; Figures 6C and 6D). This difference was abolished after application of ZD7288 (naive+ZD7288: 709 ± 73 MΩ), suggesting the initial disparity stemmed from a reduction in HCN. ZD7288 also inhibits Nav1.4[22] at an activation threshold of −40 Mv[23] and T-type Ca channels with low affinity (IC_{50} = 100 μM[24]). These channels are unlikely to contribute to the increase in R_{in} quantified at −60 mV following 20 μM ZD7288 application in naive control mice. We estimate that I_h contributes ~36% of the resting membrane conductance in cerebellar SCs and that this inward current depolarizes the membrane potential in naive mice.[3] Indeed, when voltage was measured immediately after cell break-in, neurons from naive animals exhibited a more depolarized membrane potential (−60 ± 0.9 mV) than those from FC animals (−68 ± 2.6 mV; Holm-Sidak post hoc: $t = -3.34$, $p = 0.002$; Figure 6E). This difference was abolished when ZD7288 was present, with I_h inhibition selectively hyperpolarizing the RMP in naive but not conditioned mice. These findings suggest that fear learning produces a marked increase in stellate cell R_{in} and a more hyperpolarized resting potential due to loss of I_h.

Hyperpolarizing input evokes a depolarizing conductance via activation of HCN, reducing membrane resistance and countering the effect of inhibitory synaptic input on membrane potential.[3] To test whether I_h loss after learning enhances the SC response toa hyperpolarizing stimulus, we delivered a series of bidirectional current ramps lasting 1,000 ms and ranging from −50 to −150 pA in amplitude. Measurement of peak hyperpolarization revealed a larger voltage change in SCs from FC relative to naive mice (two-way RM ANOVA: $F_{1,13} = 25.3$, $p = 0.0002$; Figures 6F and 6G). I_h blockade with ZD7288 potentiated the voltage deflection in naive animals and produced a peak amplitude that was comparable to that observed in FC animals, demonstrating HCN-mediated opposition to membrane hyperpolarization. Many neurons display a rebound depolarization following hyperpolarizing input that evokes an increase in firing rate. In cerebellar SCs, when we examined the instantaneous spike frequency that occurred on the positive phase of the ramp and compared it to pre-ramp activity, we found that −150-pA injections elicited a greater change in action potential firing in FC (45% ± 13%) vs. naive (17% ± 7%) animals (Holm-Sidak post hoc: $p = 0.02$; Figure 6H). Blockade of I_h in naive animals increased the ramp-induced change in action potential frequency by 52% ± 10% closer to that observed in FC animals but failed to further elevate post-ramp firing in FC cells. Thus, the learning-induced reduction in I_h enhances the response of SCs to hyperpolarizing ramp input and endows SCs with a state-dependent integrative property.

Reduction of I_h increases the intrinsic excitability of cerebellar SCs

We expected that the loss of I_h following learning and increase in SC input resistance would result in more rapid depolarization of the cell membrane. Because the amplitude of unitary excitatory synaptic currents in SCs is 40–50 pA,[25] we evaluated spike output in response to a 45-pA depolarizing current step (Figures 7A–7C). In naive mice, I_h inhibition markedly reduced the first-spike latency when compared to recordings made without ZD7288 (Figure 7B), suggesting I_h activated at rest could delay action potential firing in response to

depolarizing currents. The learning-induced decrease in SC I_h also shortened the time to first spike by 42% relative to naive cells (Holm-Sidak post hoc: $p = 0.024$)—a change that was comparable to the ZD7288-mediated decrease in latency. As expected, naive SCs displayed an over 3-fold increase in action potential firing following the 45-pA depolarizing current step, with I_h blockade further enhancing spike frequency by 25% (Figure 7C). In cells from conditioned mice, depolarizing current injection elicited a nearly 4-fold increase in spike activity, the frequency of which was significantly higher than that of naive cells (Tukey's post hoc: $p = 0.028$), a difference that was lost in the presence of ZD7288 (Tukey's post hoc: $p = 0.25$); I_h inhibition did not further increase evoked action potential frequency in these cells. Since basal firing rates did not differ between groups, our findings suggest that the FC-induced decrease in I_h is responsible for the enhanced SC response to depolarizing input.

We next tested whether an increase in neuronal excitability would augment SC output following a burst of presynaptic parallel fiber activity (Figure 7D). Firing frequency within the first 100 ms after parallel fiber stimulation was measured and a threshold response—defined as three standard deviations greater than the basal firing rate—was determined. We found that fear learning significantly lowered the threshold at which cells responded (Nv 7.7 ± 1.2 mV vs. FC 4.3 ± 0.6 mV, $p = 0.025$). At the 6-V stimulation intensity, firing rate of the FC group was 2-fold greater than that of the naive group, while basal frequency did not differ between the two conditions (Figure 7F). The average ratios corresponding to the change in firing between baseline and near-threshold intensity (6 V) were 6.3 and 10.7 in naive and FC recordings, respectively. Since the changes in frequency elicited by a 45-pA step injection were 4.9 and 7.0 in naive and FC recordings (Figure S5), respectively, increased intrinsic excitability following fear learning can in part account for the enhanced SC response to synaptic input. Thus, FC results in increased SC output at the parallel fiber synapse, lowering the threshold for action potential generation and increasing the neuronal firing response.

DISCUSSION

Considering the extensive connections formed between the cerebellum and the limbic system, one fundamental question is whether the cerebellar circuit encodes memory formation processes or simply serves as a relay station. Neural plasticity is the cellular substate of memory traces and involves changes in both synaptic transmission and intrinsic membrane properties. An increase in intrinsic excitability can amplify neural responses to synaptic inputs, promote action potential firing, and optimize information processing within a neuronal circuit. Thus, a long-standing objective has been to determine how learning-induced plasticity in intrinsic excitability is achieved. In the current study, we found that silencing MLIs in lobules V/VI abolished memory consolidation, revealing cerebellar inhibitory interneuron activity as a key component of memory formation. Associative FC induced a lobule-specific decrease in I_h amplitude, and the loss of HCN produced an increase in SC R_{in} and enhanced response to excitatory and inhibitory inputs. We showed that the reduction in I_h was caused by a decrease in eCB signaling, as activation of CB1Rs via the $G_{\beta\gamma}$-JNK-NOS-cGMP pathway restored current amplitude in conditioned mice. Moreover, eCB release from PCs, which is known to disrupt memory consolidation,[10]

prevented the learning-induced decrease in HCN currents. Our findings show that learning can modify functional HCN through a change in tonic eCB signaling and thereby SC intrinsic excitability, driving memory consolidation processes in the cerebellum.

The cerebellar vermis plays an important role in defensive responses and the formation of associative fear memory.[8,10] Lesions to this structure attenuate a variety of fear-related behaviors, whereas vermal stimulation elicits defensive responses.[9,26] Reversible inactivation of the vermis has been shown to disrupt the consolidation of associative fear memory.[8,27,28] Using cell-type and lobule-specific chemogenetic manipulation, we determined that inhibitory interneuron activity within lobules V/VI drives memory consolidation in the cerebellum. Importantly, learning-induced changes in SC I_h were also observed in lobules V/VI but not in lobule IX, which receives afferents from the peripheral vestibular end organs.[29] At the circuit level, FC selectively increases both excitatory and inhibitory synaptic transmission onto PCs and strengthens inhibitory connectivity in lobules V/VI.[11–13] Our recent mechanistic study revealed that FC elevates MAGL levels, accelerates 2-AG degradation, and reduces eCB signaling in a lobule-specific manner.[10] These findings agree with the involvement of V/VI lobules in FC. Reduction in I_h and the resultant increase in SC excitability could underlie the previously reported enhancement of feedforward inhibition onto PCs after FC,[12] modifying their activity during associative memory processes.

The reduction in SC I_h observed after fear learning produced large alterations in neuronal response to both hyperpolarizing and depolarizing current injections. Decreased HCN enhanced the SC response to depolarizing inputs, which could augment the speed[30] and strength of SC inhibition onto PCs, respectively. SCs from FC animals exhibited increased propensity to fire at lower parallel fiber stimulation intensities relative to controls, revealing a reduction in the SC threshold for action potential generation. As SC-generated spikes can delay PC firing,[31] a decline in I_h may facilitate feedforward inhibition onto PCs, controlling the temporal features of conditioned responses after FC.

SCs from FC animals also exhibited greater membrane hyperpolarization and rebound activity to bidirectional current ramps, as shown in PCs when the HCN1 subunit is deleted.[6] This finding is important as a lasting increase in GABA release, such as that reported after FC,[10,12] could amplify rebound action potential firing in MLIs and profoundly impact the activity of inhibitory networks within the cerebellum. If rebound bursts occur simultaneously across neighboring SCs, a learning-induced reduction in HCN may enhance their degree of synchrony to form more extensive, coherent signals onto target PCs. In agreement with this, *in vivo* recordings show that interneuron synchrony strengthens the inhibition of PC firing.[32] SCs with high R_{in} are also more likely to be electrically coupled to neighboring cells, boosting the probability of synchronized firing.[33] Given that loss of I_h conductance increases SC input resistance, networks of electronically coupled SCs that give rise to synchronized activity may form after associative learning.

In the context of learning and memory, augmented intrinsic excitability can alter the temporal integration of synaptic events—and thereby the output of a neuronal circuit—and reduce the threshold for the induction of other forms of synaptic plasticity. These changes

could enhance the likelihood that neurons will be engaged in encoding memories or enable their selective reactivation during post-training periods.[34–40] Indeed, we found that silencing MLIs after FC was sufficient to completely disrupt memory consolidation, highlighting the important role of cerebellar interneuron activity in the formation of associative fear memory.

The resting I_h conductance in MLIs from naive animals represents ~36% of resting membrane conductance. Thus, resting I_h is likely to contribute to the instantaneous current only in naive animals, as learning reduces I_h in MLIs. The instantaneous current at −100 mV, the K equilibrium potential, decreased from −77 ± 8.4 pA in naive controls to −37 ± 0.6 pA following fear conditioning ($p = 0.0002$). This difference was lost when the resting I_h component, estimated using a reversal potential of −40 mV, was subtracted from the total instantaneous current in control mice ($p = 0.42$). Such a result was also found at −120 mV (Figure S7). Therefore, a decrease in resting I_h after fear conditioning can account for the difference in instantaneous current between naive and conditioned mice.

cGMP and cAMP stimulate HCN channels and cause a depolarizing shift in activation, enhancing I_h.[41–43] CB1R agonism has been shown to produce similar changes in I_h in a subset of CA1 neurons via $G_{\beta\gamma}$-JNK-NOS-cGMP.[19] We found that HCN channels in SCs are also highly sensitive to CB1R signaling and that tonic eCB promotes I_h in naive animals. As in CA1 neurons, we observed that NO in cerebellar SCs mediates a cGMP-dependent increase in I_h via $G_{\beta\gamma}$-JNK following CB1R activation. This suggests eCB acts as a common neuromodulator to gate HCN currents through regulation of cGMP. One fundamental question is whether an experience, such as learning, can modify HCN activity and thereby intrinsic excitability through regulation of eCB signaling. We recently showed that learning reduces eCBs in cerebellar lobules V/VI[10] and that this decrease is critical for memory formation. Here, we demonstrate that FC diminishes I_h amplitude and that CB1R agonism can fully rescue that loss. While eCB signaling also regulates a K^+ conductance in cerebellar SCs,[44] the loss in I_h can fully explain the changes in intrinsic excitability observed after FC. In addition to I_h, eCBs also directly interact with Kv7 channels in hippocampal interneurons, inducing a long-lasting suppression of intrinsic excitability.[45] Therefore, eCBs can control the intrinsic excitability of neurons via both CB1R-dependent and -independent mechanisms.

The learning-induced decrease in tonic eCB and resulting reduction in SC I_h after learning corresponded to an increase in synaptic transmission[10] and cerebellar interneuron excitability. This form of plasticity has behavioral consequences, as eCB release from PCs has been shown to disrupt memory consolidation.[10] Accordingly, we found that chemogenetic release of PC eCBs could prevent FC-related disruptions in I_h. Since cerebellar interneuron activity is essential for memory consolidation, these results suggest that eCB-mediated HCN plasticity is critically involved in the formation of fear memory, in part through an increase in intrinsic excitability and synaptic activity.

HCN channels exhibit distinct subcellular localization that strongly influences the role of I_h.[46–50] I_h in inhibitory interneurons of the cortex and hippocampus appears chiefly somatic, exerting an influence on excitability through depolarization of the resting potential and the generation of rhythmic action potentials.[51] The presence of I_h in the synaptic terminals and

somata of cerebellar basket cells[15,52,53] implicates a role for HCN in regulating interneuron excitability and GABA release onto PCs, which could modify their activity and ultimate output. In contrast, in CA1 pyramidal neurons, the 6- to 8-fold greater appearance of I_h in distal apical dendrites versus the soma[6,18,54,55] is important in attenuating synaptic potentials. Neuronal activity, such as theta bursting in the hippocampus[34] and a single seizure episode in the entorhinal cortex,[56] can also bring about changes in I_h. Similarly, activity-dependent changes in eCB signaling may contribute to HCN plasticity in other brain regions under physiological and pathological conditions. Given eCB signaling is cell-type specific, mechanisms underlying HCN plasticity are likely to be circuit dependent.

Overall, our results reveal that a sustained, learning-dependent change in tonic eCB signaling gates HCN channels and resets membrane excitability. This form of plasticity occurs selectively in cells that express both HCN channels and CB1Rs and requires an activity-dependent change in eCBs. Alteration of this neuromodulator can produce and synchronize multiple forms of plasticity, at both the synapse and the membrane, presenting a powerful mechanism to amplify the output of a neural circuit and drive memory formation. Considering eCB signaling can also be modified by drug abuse and under pathological conditions, it is highly plausible that eCB-HCN plasticity has broader functional impact on a range of behaviors. Our findings highlight the importance of cerebellar inhibitory interneuron activity and modulation of their intrinsic excitability in behaviorally complex processes like memory consolidation.

Limitations of the study

In this study, we recorded I_h from MLIs in the upper 2/3 of the molecular layer, presumably SCs in lobules V/VI of the cerebellar vermis. The effects of fear conditioning on HCN channel activity in other cerebellar neurons, basket cells, Golgi cells, and PCs remain to be determined. While PCs also express HCN channels, eCB receptors are absent in these neurons and therefore are unlikely to undergo the same type of HCN plasticity as in cerebellar SCs. Thus, our study does not suggest that the learning-induced reduction of HCN channels specifically occurs in SCs. This study focuses on learning-induced changes in I_h, and we did not quantify currents of other resting channels and voltage-gated ion channels. Therefore, while changes in intrinsic excitability can be explained by learning-induced alterations in I_h, we cannot rule out contributions from other ion channels.

STAR★METHODS

RESOURCE AVAILABILITY

Lead contact—Further information and requests for resources and reagents should be directed to and will be fulfilled by the lead contact, Siqiong June Liu (sliu@lsuhsc.edu).

Materials availability—The study did not generate any new unique reagents or materials.

Data and code availability

- Source data for each figure are available in Table S2.

- This paper does not report original code.
- Any additional information required to reanalyze the data reported in this paper is available from the lead contact upon request.

EXPERIMENTAL MODEL AND SUBJECT DETAILS

Animals—C57Bl/6 background mice were purchased from Jackson Laboratory (Bar Harbor, ME). Breeding colonies were established and maintained in our animal facility (C57Bl/6J wild-type stock 000664). An L7-cre mouse line (B6.129-Tg(Pcp2-cre)2Mpin/J) (stock 004146) was crossed with floxed Gq-DREADD (Gt(ROSA)26Sortm2 (CAG-CHRM3*,-mCitrine)Ute/J) (stock 026220, hemizygous) to generate L7:hM3Dq(+) and L7:hM3Dq(−) mutant mice, referred as L7:Gq(+) and L7:Gq(−) mice in the results section, respectively. Our previous study confirmed the expression and function of hM3Dq in cerebellar PCs, as mCitrine fluorescence was detected only in PCs of brain sections prepared from double mutant mice and CNO application selectively altered PC activity in the cerebellar cortex.[10]

Both female and male mice (P18–90) were used in this study. Experiments quantifying the effects of CNO on I_h in L7:Gq(+) and L7:Gq(−) mice were conducted only in P60–90 male mice to match the behavioral experiments described in our previous publication.[10] Currents recorded in these mice were indistinguishable from those obtained using P18–60 mice.

Breeding colonies were maintained on a 12 h light/dark cycle, with *ad libitum* food and water supply. Animals were group housed. Experimental procedures were conducted in accordance with the Louisiana State University Health Sciences Center's guidelines for the care and use of laboratory animals.

METHOD DETAILS

Fear conditioning—C57BL/6J mice of either sex (N = 109) were divided into four groups: fear conditioned, unpaired, and naive. Mice in the conditioned group underwent a delayed fear learning paradigm during which they were placed inside a conditioning apparatus (constructed in-house) and left undisturbed for 2 min (baseline). After this time, eight 10 s long acoustic stimuli (conditioned stimulus; 75 dB, 3.5-kHz tone) were administered at 30 s intervals. The last 1 s of each conditioned stimulus was paired with an unconditioned stimulus, which consisted of an electric foot shock (0.75 mA). The second group of mice (unpaired) underwent a non-associative control procedure in which the foot shock and tone were explicitly unpaired. During this procedure, mice were placed in the above-described apparatus and received the same number of acoustic stimuli at 30 s intervals. Mice were returned to their home cage for 30 min, after which they were placed back in the apparatus, where they received a series of eight unconditioned stimuli at 30-s intervals. These procedures were designed to make it difficult for mice to associate the unconditioned and conditioned stimulus. Mice in both conditioned and unpaired groups were sacrificed one day after acquisition for electrophysiological recordings. Mice in the naive group never left their home cage. In all experimental groups, a video camera mounted on the top of each chamber was used to record activity during behavioral testing. To assess learning, freezing response was measured as the percentage of immobility during baseline,

the eight 9-s stretches of conditioned stimulus before presentation of the unconditioned stimulus (acquisition), and the 1-min period immediately after the acquisition phase. Freezing was defined as the complete absence of motility with the exception of respiratory movement. Freezing responses during learning in all animals were greater than average basal freezing +10xSD. There were no correlations between memory retention and % freezing during learning among control groups (mCherry + CNO, GiDREADD + saline and GiDREADD injected to lobule VII + CNO, n = 15) and in GiDREADD in lobules V/VI + CNO (n = 6) (Figure S1).

In experiments using GqDREADD animals, both L7:Gq(+) and L7:Gq(−) mice were subjected to a fear conditioning paradigm and received CNO (0.5 mg/kg) 30 min later. Electrophysiological recordings were performed the next day.

Electrophysiology: Slice preparation—Horizontal and sagittal cerebellar slices (thicknesses of 400 and 300 mm, respectively) were cut from the brains of C57BL/6J or L7:Gq(+ or −) mice in ice-cold sucrose slicing solution (in mM: NaCl 81.2, KCl 2.4, $NaHCO_3$ 23.4, NaH_2PO_4 1.4, $CaCl_2$ 0.5, $MgCl_2$ 6.7, sucrose 69.9, and glucose 23.3, oxygenated with a 5% CO_2/95% O_2 mix) using a VT1000S vibrating microslicer (Leica Biosystems, Bannockburn, Ill). After sectioning, slices were transferred to a recording chamber where they were perfused with oxygenated external solution (in mM: NaCl 125, KCl 2.5, $NaHCO_3$ 26, NaH_2PO_4 1.25, $CaCl_2$ 2, $MgCl_2$ 1, and glucose 25, pH 7.4). SCs were visually identified in the upper two-thirds of the molecular layer and confirmed electrophysiologically by the presence of spontaneous spiking activity. Current- and voltage-clamp recordings were made with an Axopatch 200B amplifier (Axon Instruments, Foster City, CA), and patch pipettes were pulled from standard-walled borosilicate glass tubing. When filled with internal solution, the resistance of the patch pipettes was 6–8 MΩ. Membrane current and voltage were sampled at 10 kHz and low-pass filtered at 2 kHz.

Voltage-clamp recordings and analysis of HCN currents—Whole cell, voltage-clamp recordings were performed at a temperature of 21°C–24°C (unless stated otherwise), using a potassium-based internal solution containing the following (in mM): KCl 135, K-EGTA 1, $MgCl_2$ 4.6, $CaCl_2$ 0.1, HEPES 10, ATP-Na 4, and GTP-NA 0.4; pH adjusted to 7.25 with KOH. Cells were held at a potential of −60 mV. Series resistance was monitored over the duration of all voltage-clamp recordings, and collected data were not included if this value changed by more than 30%. Only cells with a holding current of less than −100 pA were included in the final dataset. To characterize I_h, 100 μM picrotoxin and 1 mM kynurenic acid were included in the bath solution; 0.3 mM tetrodotoxin was added after the confirmation of spontaneous spiking activity. Input resistance (R_{in}) was determined by measuring the response of the steady-state current to a 5-mV hyperpolarizing pulse (from −60 to −65 mV, 50-ms duration). I_h was evoked by delivering a series of 1-*s*-long hyperpolarizing voltage steps, from −50 to −120 mV in 10-mV increments. The amplitude of I_h was measured as the difference between currents in the presence and absence of the HCN channel blockers, ZD7288 (20 μM) or CsCl (1 mM); ZD7288 effects were assessed 10 min after its application. As HCN channels exhibit slow activating inward currents, I_h amplitude was also quantified as the difference between the steady-state slowly

activating current and the instantaneous current. Activation kinetics were determined by fitting the onset of the current with a single exponential function: $f(t) = Ae^{-(t/t)}+C$. To assess voltage-sensitivity, half-maximal activation (V_{50}) was determined by fitting individual conductance-voltage (G–V) relationships with a Boltzmann function: $G/G_{max} = A2+(A1–A2)/\{1+[\exp(x–x_0)/dx]\}$, where G_{max} is the mean value of the fit maximal conductance, x_0 is the membrane potential for half-maximal activation of the current (V_{50}), and dx is the slope factor. Using a previously reported reversal potential for I_h in MLIs,[15] we quantified G as I_h amplitude/(V_m–reversal potential). We observed no difference between I_h amplitude in stellate cells from P18–30 (n = 11; −68.0 ± 5.7 pA; Figure S2) and P30–60 (n = 8; −58.4 ± 4.1 pA; unpaired t test: $t_{17} = 1.3$, p = 0.12; Figure S6A) naive mice. Fear conditioning reduced the amplitude of I_h in both age groups (n = 5/group; <1-month-old, −23.9 + 1.6 pA; >1 month: −24.0 ± 2.4 pA; unpaired t test: $t_{12} = −0.049$, p = 0.96; Figure S6B) and has been shown to attenuate endocannabinoid signaling in P18—110 mice.[10] Thus, experiments determining the effects of eCBs on I_h (Figures 3–6) were performed in 4- to 12-week-old mice. The liquid junction potential was 4.3 mV when calculated using Clampex and was not compensated.

Current clamp recordings and analysis of action potential firing—All current-clamp and cell-attached recordings were conducted at near physiological temperature (34–37°C). For current-clamp experiments, internal solution contained (in mm) 115 $KMeSO_3$, 10 HEPES, 0.5 K-EGTA, 0.16 $CaCl_2$, 2 $MgCl_2$, 10 NaCl, 4 ATP-Na, 14 Tris-creatine phosphate, 0.4 GTP-Na. Resting membrane potential was measured immediately after obtaining access to the cell interior. Membrane potential was maintained by injecting a constant negative holding current (≤20 pA) for the duration of the recording. I_h sag was measured as the difference between the peak hyperpolarization produced by a current step of −75 pA and the amplitude of the steady-state potential at the end of the current step. For ramp experiments, data was divided into 30 × 100-ms epochs for which the mean spike frequency across all epochs was calculated. An average of the epochs before the ramp was used as the baseline frequency while mean action potential frequency within the first two epochs after the ramp (200-ms) was categorized as instantaneous frequency. The percent difference in mean spike frequency was then calculated for the two time points. In current clamp analyses, we removed a recording from one neuron in the naive condition whose data was ≥3 SDs higher than the mean value for all parameters measured.

Parallel fiber stimulation and cell-attached recordings—To determine the SC response to physiologically relevant excitatory input, patch pipettes were filled with extracellular perfusion solution and a loose seal (<100 MΩ) was obtained. A glass microelectrode (tip diameter, ~10 μm) was then placed in the molecular layer ≥100 μm from the recording electrode to evoke parallel fiber activity. Action potentials were continuously recorded in current clamp mode with 0 pA current injection. The stimulation protocol consisted of a burst of four pulses of equal intensity (200-μsec duration) delivered at 100 Hz, and the stimulation intensity changed between 2 and 20 V in 2-V increments or decrements between trials. The protocol, which lasted 10 min (1-min/sweep), was repeated two to four times, and the location of the stimulation pipette tip was carefully monitored during experiments; recordings were terminated if a shift in position was observed. In order to

eliminate the inhibitory influence of other SCs on the recorded cell, 100 μM picrotoxin and 20 μM SR 95531 were bath-applied during all cell-attached recordings.

Stereotaxic surgeries and viral injection—Adeno-associated viruses (AAV) pAAV-hSyn-DIO-hM4D(Gi)-mCherry and pAAV-hSyn-DIO-mCherry were purchased from Addgene (Watertown, USA). nNos-Cre homozygous mice (~P24–P90) were anesthetized with isoflurane and placed in a stereotaxic frame (Neurostar). For viral injections, a glass electrode filled with AAV virus was placed into the target area according to the corresponding coordinates: Lobules V/VI inclusive (lambda 15–20 mm posterior, 0 mm M/L, 2 mm ventral) and Lobules V/VI exclusive (Lambda ± ~35 mm posterior, ±0 mm M/L, 2 mm ventral). The scalp incision was stapled, and animals were allowed at least 2 weeks to recover and express the virus before FC training (tone + shock in context A) and memory retention tests (tone alone in context B, conducted 24 h after FC). Freezing responses to tones were quantified as described above. Correct location of the virus injection was confirmed postmortem by mCherry fluorescence.

QUANTIFICATION AND STATISTICAL ANALYSIS

Data are presented as mean ± SEM. All data were analyzed using clampfit, SigmaPlot, Origin-Pro, and Excel software. Means of three or more groups collected from separate neurons were analyzed using a one- or two-way analysis of variance (ANOVA). Where indicated, a two-way repeated measures (RM) ANOVA was used to determine the effect of treatment (e.g., naive vs. FC) on peak current in response to varying injected voltage steps (i.e., −120 to −50 mV). Means of three or more groups were analyzed using a one-way ANOVA. A Holm-Sidak or Tukey post-hoc test was run for multiple comparisons. The significance level for all tests was set at $p < 0.05$, and n presents number of animals in Figures 1A–1D and number of cells in other experiments. The statistical details were indicated in the figure legends, figures and described in the Results section. A summary of statistical analysis is available in Table S1.

Supplementary Material

Refer to Web version on PubMed Central for supplementary material.

ACKNOWLEDGMENTS

This work was supported by grants from the National Institutes of Health (NIH; R01MH095948 and R01 NS106915 to S.J.L.; F32MH103964 to K.L.C.), a grant from The Brown Foundation (611019, to G.K.), and a grant from the Department of Veterans Affairs (I01 BX003893–01A1). We would like to thank Drs. Matthew Whim, Sonia Gasparini, and Christophe Dubois for technical assistance and for providing invaluable feedback on this project.

REFERENCES

1. Malone TJ, and Kaczmarek LK (2022). The role of altered translation in intellectual disability and epilepsy. Prog. Neurobiol 213, 102267. [PubMed: 35364140]
2. Alexander RPD, and Bowie D (2021). Intrinsic plasticity of cerebellar stellate cells is mediated by NMDA receptor regulation of voltage-gated Na+ channels. J. Physiol 599, 647–665. [PubMed: 33146903]

3. Kase D, and Imoto K (2012). The Role of HCN Channels on Membrane Excitability in the Nervous System. J. Signal Transduct 2012, 619747. [PubMed: 22934165]
4. Nolan MF, Malleret G, Dudman JT, Buhl DL, Santoro B, Gibbs E, Vronskaya S, Buzsáki G, Siegelbaum SA, Kandel ER, and Morozov A (2004). A behavioral role for dendritic integration: HCN1 channels constrain spatial memory and plasticity at inputs to distal dendrites of CA1 pyramidal neurons. Cell 119, 719–732. [PubMed: 15550252]
5. Rinaldi A, Defterali C, Mialot A, Garden DLF, Beraneck M, and Nolan MF (2013). HCN1 channels in cerebellar Purkinje cells promote late stages of learning and constrain synaptic inhibition. J. Physiol 591, 5691–5709. [PubMed: 24000178]
6. Nolan MF, Malleret G, Lee KH, Gibbs E, Dudman JT, Santoro B, Yin D, Thompson RF, Siegelbaum SA, Kandel ER, and Morozov A (2003). The hyperpolarization-activated HCN1 channel is important for motor learning and neuronal integration by cerebellar Purkinje cells. Cell 115, 551–564. [PubMed: 14651847]
7. Maschke M, Schugens M, Kindsvater K, Drepper J, Kolb FP, Diener HC, Daum I, and Timmann D (2002). Fear conditioned changes of heart rate in patients with medial cerebellar lesions. J. Neurol. Neurosurg. Psychiatry 72, 116–118. [PubMed: 11784838]
8. Sacchetti B, Baldi E, Lorenzini CA, and Bucherelli C (2002). Cerebellar role in fear-conditioning consolidation. Proc. Natl. Acad. Sci. USA 99, 8406–8411. [PubMed: 12034877]
9. Supple WF, and Leaton RN (1990). Lesions of the cerebellar vermis and cerebellar hemispheres: effects on heart rate conditioning in rats. Behav. Neurosci 104, 934–947. [PubMed: 2285492]
10. Dubois CJ, Fawcett-Patel J, Katzman PA, and Liu SJ (2020). Inhibitory neurotransmission drives endocannabinoid degradation to promote memory consolidation. Nat. Commun 11, 6407. [PubMed: 33335094]
11. Sacchetti B, Scelfo B, Tempia F, and Strata P (2004). Long-term synaptic changes induced in the cerebellar cortex by fear conditioning. Neuron 42, 973–982. [PubMed: 15207241]
12. Scelfo B, Sacchetti B, and Strata P (2008). Learning-related long-term potentiation of inhibitory synapses in the cerebellar cortex. Proc. Natl. Acad. Sci. USA 105, 769–774. [PubMed: 18184813]
13. Ruediger S, Vittori C, Bednarek E, Genoud C, Strata P, Sacchetti B, and Caroni P (2011). Learning-related feedforward inhibitory connectivity growth required for memory precision. Nature 473, 514–518. [PubMed: 21532590]
14. Zhu L, Scelfo B, Tempia F, Sacchetti B, and Strata P (2006). Membrane excitability and fear conditioning in cerebellar Purkinje cell. Neuroscience 140, 801–810. [PubMed: 16580140]
15. Saitow F, and Konishi S (2000). Excitability increase induced by beta-adrenergic receptor-mediated activation of hyperpolarization-activated cation channels in rat cerebellar basket cells. J. Neurophysiol 84, 2026–2034. [PubMed: 11024095]
16. Huang CM, Liu G, and Huang R (1982). Projections from the cochlear nucleus to the cerebellum. Brain Res 244, 1–8. [PubMed: 7116161]
17. Snider R, and Stowell A (1944). RECEIVING AREAS OF THE TACTILE, AUDITORY, AND VISUAL SYSTEMS. In THE CEREBELLUM (undefined)
18. Santoro B, Liu DT, Yao H, Bartsch D, Kandel ER, Siegelbaum SA, and Tibbs GR (1998). Identification of a gene encoding a hyperpolarization-activated pacemaker channel of brain. Cell 93, 717–729. [PubMed: 9630217]
19. Maroso M, Szabo GG, Kim HK, Alexander A, Bui AD, Lee SH, Lutz B, and Soltesz I (2016). Cannabinoid Control of Learning and Memory through HCN Channels. Neuron 89, 1059–1073. [PubMed: 26898775]
20. Oberdick J, Smeyne RJ, Mann JR, Zackson S, and Morgan JI (1990). A promoter that drives transgene expression in cerebellar Purkinje and retinal bipolar neurons. Science 248, 223–226. [PubMed: 2109351]
21. Altomare C, Terragni B, Brioschi C, Milanesi R, Pagliuca C, Viscomi C, Moroni A, Baruscotti M, and DiFrancesco D (2003). Heteromeric HCN1-HCN4 channels: a comparison with native pacemaker channels from the rabbit sinoatrial node. J. Physiol 549, 347–359. [PubMed: 12702747]

22. Wu X, Liao L, Liu X, Luo F, Yang T, and Li C (2012). Is ZD7288 a selective blocker of hyperpolarization-activated cyclic nucleotide-gated channel currents? Channels 6, 438–442. [PubMed: 22989944]

23. Männikkö R, Wong L, Tester DJ, Thor MG, Sud R, Kullmann DM, Sweeney MG, Leu C, Sisodiya SM, FitzPatrick DR, et al. (2018). Dysfunction of NaV1.4, a skeletal muscle voltage-gated sodium channel, in sudden infant death syndrome: a case-control study. Lancet 391, 1483–1492. [PubMed: 29605429]

24. Felix R, Sandoval A, Sánchez D, Gómora JC, De la Vega-Beltrán JL, Treviñ o CL, and Darszon A (2003). ZD7288 inhibits low-threshold Ca(2+) channel activity and regulates sperm function. Biochem. Biophys. Res. Commun 311, 187–192. [PubMed: 14575712]

25. Liu Y, Formisano L, Savtchouk I, Takayasu Y, Szabó G, Zukin RS, and Liu SJ (2010). A single fear-inducing stimulus induces a transcription-dependent switch in synaptic AMPAR phenotype. Nat. Neurosci 13, 223–231. [PubMed: 20037575]

26. Snider RS, and Maiti A (1976). Cerebellar contributions to the Papez circuit. J.. Res 2, 133–146.

27. Neurosci Sacchetti B, Sacco T, and Strata P (2007). Reversible inactivation of amygdala and cerebellum but not perirhinal cortex impairs reactivated fear memories. Eur. J. Neurosci 25, 2875–2884. [PubMed: 17466022]

28. Yoshida M, and Hirano R (2010). Effects of local anesthesia of the cerebellum on classical fear conditioning in goldfish. Behav. Brain Funct 6, 20. [PubMed: 20331854]

29. Barmack NH, and Yakhnitsa V (2013). Modulated discharge of Purkinje and stellate cells persists after unilateral loss of vestibular primary afferent mossy fibers in mice. J. Neurophysiol 110, 2257–2274. [PubMed: 23966673]

30. Mittmann W, Koch U, and Häusser M (2005). Feed-forward inhibition shapes the spike output of cerebellar Purkinje cells. J. Physiol 563, 369–378. [PubMed: 15613376]

31. Häusser M, and Clark BA (1997). Tonic synaptic inhibition modulates neuronal output pattern and spatiotemporal synaptic integration. Neuron 19, 665–678. [PubMed: 9331356]

32. Blot A, de Solages C, Ostojic S, Szapiro G, Hakim V, and Léna C (2016). Time-invariant feed-forward inhibition of Purkinje cells in the cerebellar cortex in vivo. J. Physiol 594, 2729–2749. [PubMed: 26918702]

33. Mann-Metzer P, and Yarom Y (1999). Electrotonic coupling interacts with intrinsic properties to generate synchronized activity in cerebellar networks of inhibitory interneurons. J. Neurosci 19, 3298–3306. [PubMed: 10212289]

34. Fan Y, Fricker D, Brager DH, Chen X, Lu HC, Chitwood RA, and Johnston D (2005). Activity-dependent decrease of excitability in rat hippocampal neurons through increases in I(h). Nat. Neurosci 8, 1542–1551. [PubMed: 16234810]

35. Disterhoft JF, and Oh MM (2006). Learning, aging and intrinsic neuronal plasticity. Trends Neurosci 29, 587–599. [PubMed: 16942805]

36. Mozzachiodi R, and Byrne JH (2010). More than synaptic plasticity: role of nonsynaptic plasticity in learning and memory. Trends Neurosci 33, 17–26. [PubMed: 19889466]

37. Zhang W, and Linden DJ (2003). The other side of the engram: experience-driven changes in neuronal intrinsic excitability. Nat. Rev. Neurosci 4, 885–900. [PubMed: 14595400]

38. Gouty-Colomer LA, Hosseini B, Marcelo IM, Schreiber J, Slump DE, Yamaguchi S, Houweling AR, Jaarsma D, Elgersma Y, and Kushner SA (2016). Arc expression identifies the lateral amygdala fear memory trace. Mol. Psychiatr 21, 1153.

39. Cai DJ, Aharoni D, Shuman T, Shobe J, Biane J, Song W, Wei B, Veshkini M, La-Vu M, Lou J, et al. (2016). A shared neural ensemble links distinct contextual memories encoded close in time. Nature 534, 115–118. [PubMed: 27251287]

40. Zhou Y, Won J, Karlsson MG, Zhou M, Rogerson T, Balaji J, Neve R, Poirazi P, and Silva AJ (2009). CREB regulates excitability and the allocation of memory to subsets of neurons in the amygdala. Nat. Neurosci 12, 1438–1443. [PubMed: 19783993]

41. Biel M, Wahl-Schott C, Michalakis S, and Zong X (2009). Hyperpolarization-activated cation channels: from genes to function. Physiol. Rev 89, 847–885. [PubMed: 19584315]

42. Kopp-Scheinpflug C, Pigott BM, and Forsythe ID (2015). Nitric oxide selectively suppresses IH currents mediated by HCN1-containing channels. J. Physiol 593, 1685–1700. [PubMed: 25605440]
43. Shah MM (2014). Cortical HCN channels: function, trafficking and plasticity. J. Physiol 592, 2711–2719. [PubMed: 24756635]
44. Kreitzer AC, Carter AG, and Regehr WG (2002). Inhibition of interneuron firing extends the spread of endocannabinoid signaling in the cerebellum. Neuron 34, 787–796. [PubMed: 12062024]
45. Incontro S, Sammari M, Azzaz F, Inglebert Y, Ankri N, Russier M, Fantini J, and Debanne D (2021). Endocannabinoids Tune Intrinsic Excitability in O-LM Interneurons by Direct Modulation of Postsynaptic Kv7 Channels. J. Neurosci 41, 9521–9538. [PubMed: 34620719]
46. Aponte Y, Lien C-C, Reisinger E, and Jonas P (2006). Hyperpolarization-activated cation channels in fast-spiking interneurons of rat hippocampus. J. Physiol 574, 229–243. [PubMed: 16690716]
47. Bender RA, Kirschstein T, Kretz O, Brewster AL, Richichi C, Rüschenschmidt C, Shigemoto R, Beck H, Frotscher M, and Baram TZ (2007). Localization of HCN1 channels to presynaptic compartments: novel plasticity that may contribute to hippocampal maturation. J. Neurosci 27, 4697–4706. [PubMed: 17460082]
48. Berger T, Senn W, and Lüscher HR (2003). Hyperpolarization-activated current Ih disconnects somatic and dendritic spike initiation zones in layer V pyramidal neurons. J. Neurophysiol 90, 2428–2437. [PubMed: 12801902]
49. Magee JC (1998). Dendritic hyperpolarization-activated currents modify the integrative properties of hippocampal CA1 pyramidal neurons. J. Neurosci 18, 7613–7624. [PubMed: 9742133]
50. Poolos NP, Migliore M, and Johnston D (2002). Pharmacological upregulation of h-channels reduces the excitability of pyramidal neuron dendrites. Nat. Neurosci 5, 767–774. [PubMed: 12118259]
51. Lupica CR, Bell JA, Hoffman AF, and Watson PL (2001). Contribution of the hyperpolarization-activated current (I(h)) to membrane potential and GABA release in hippocampal interneurons. J. Neurophysiol 86, 261–268. [PubMed: 11431507]
52. Luján R, Albasanz JL, Shigemoto R, and Juiz JM (2005). Preferential localization of the hyperpolarization-activated cyclic nucleotide-gated cation channel subunit HCN1 in basket cell terminals of the rat cerebellum. Eur. J. Neurosci 21, 2073–2082. [PubMed: 15869503]
53. Southan AP, Morris NP, Stephens GJ, and Robertson B (2000). Hyperpolarization-activated currents in presynaptic terminals of mouse cerebellar basket cells. J. Physiol 526, 91–97. [PubMed: 10878102]
54. Ludwig A, Zong X, Jeglitsch M, Hofmann F, and Biel M (1998). A family of hyperpolarization-activated mammalian cation channels. Nature 393, 587–591. [PubMed: 9634236]
55. Notomi T, and Shigemoto R (2004). Immunohistochemical localization of Ih channel subunits, HCN1–4, in the rat brain. J. Comp. Neurol 471, 241–276. [PubMed: 14991560]
56. Shah MM, Anderson AE, Leung V, Lin X, and Johnston D (2004). Seizure-induced plasticity of h channels in entorhinal cortical layer III pyramidal neurons. Neuron 44, 495–508. [PubMed: 15504329]
57. Chan KY, Jang MJ, Yoo BB, Greenbaum A, Ravi N, Wu WL, Sánchez-Guardado L, Lois C, Mazmanian SK, Deverman BE, and Gradinaru V (2017). Engineered AAVs for efficient noninvasive gene delivery to the central and peripheral nervous systems. Nat. Neurosci. 20, 1172–1179. [PubMed: 28671695]

Highlights

- Fear conditioning suppresses HCN currents and enhances cerebellar interneuron excitability
- A learning-induced loss of endocannabinoids drives HCN plasticity
- Activity in cerebellar interneurons controls the formation of associative fear memory

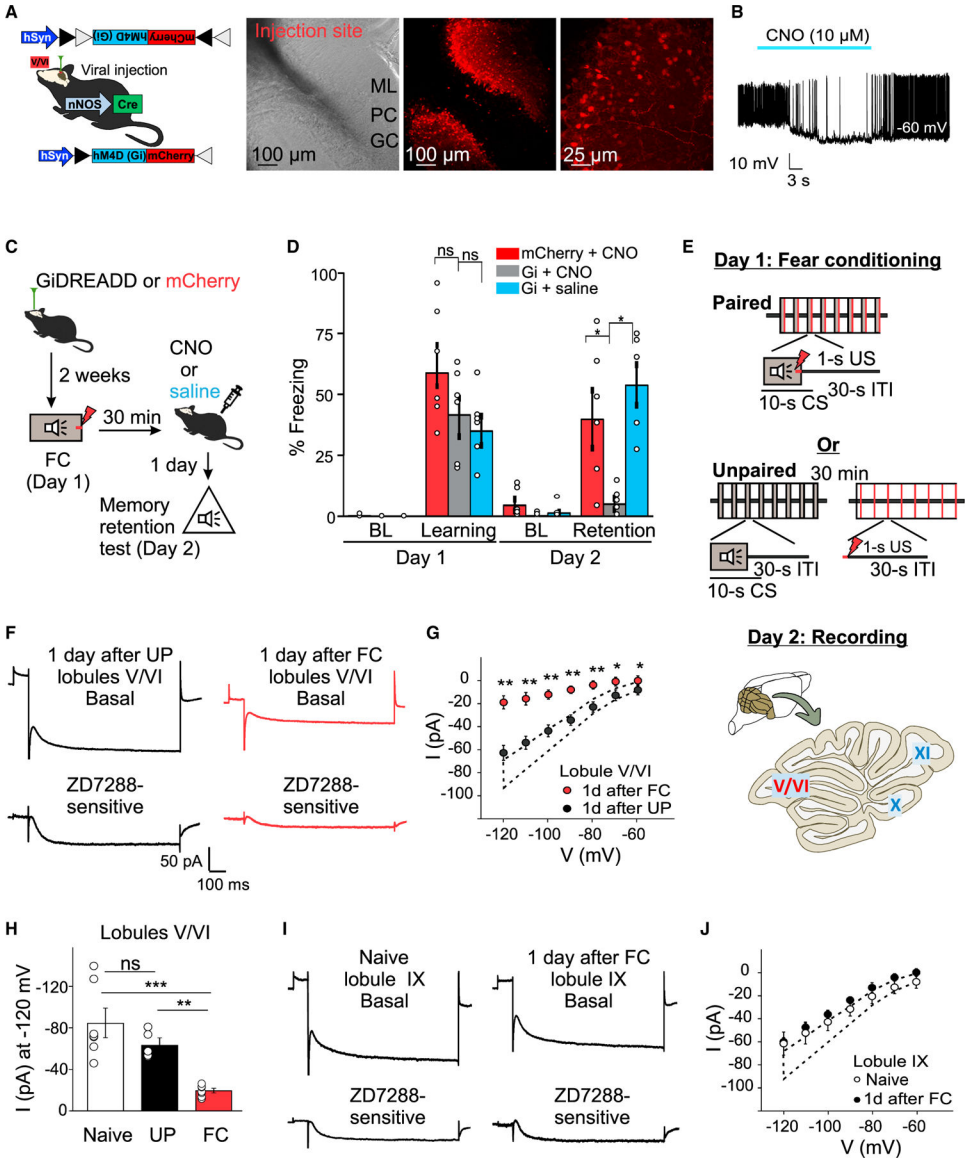

Figure 1. MLI activity drives memory consolidation, and fear conditioning selectively reduces MLI I_h in lobules V/VI

(A–D) Gi-DREADD-mediated silencing of MLIs in vermal lobules V/VI abolished memory consolidation of associative fear learning. (A) Left: experimental approach. Cre-dependent Gi-DREADD was injected into the cerebellum of nNos-cre mice to restrict Gi-DREADD expression to the molecular layer interneurons. Right: mCherry expression was detected only in cells located in the molecular layer. (B) Cell-attached recordings in an mCherry-expressing neuron in the molecular layer showed spontaneous activity, a characteristic of MLIs. Application of CNO caused membrane hyperpolarization and suppressed spontaneous action potential firing in MLIs. (C and D) Two weeks following viral injection (Gi-DREADD or mCherry), mice were subjected to fear conditioning training and received a CNO or saline injection 30 min later. Memory retention was tested the next day. Administration of CNO abolished memory retention in animals expressing Gi-DREADD in lobules V/VI but not in those expressing mCherry (without Gi-DREADD). Saline injection

in Gi-DREADD mice did not affect memory retention (n = 6/condition; two-way RM ANOVA: genotype × behavior interaction, $F_{2,15} = 5.76$, $p = 0.014$). Bonferroni post hoc: *p < 0.002. (See Figure S1).

(E–H) Fear conditioning reduced stellate cell I_h.

(E) Behavioral delay FC paradigm. Mice were presented with a tone (conditioned stimulus), followed by a temporally contiguous foot shock (unconditioned stimulus). In the unpaired, control paradigm, a tone and foot shock were explicitly unpaired. Bottom, schematic diagram of the cerebellum.

(F) Whole-cell voltage-clamp recording revealing similar peak steady-state amplitudes recorded from cells in unpaired (left panel) and paired groups (right panel).

(G) Current-voltage relationship showing that I_h amplitude was significantly reduced when FC (n = 7) and unpaired (n = 5) recordings were compared (two-way RM ANOVA: $F_{7,70} = 42.06$, $p < 0.001$ [black dashed line represents SEM for the current/voltage relationship of naive recordings presented in Figure S2B]). Tukey's post hoc: **p < 0.001, *p < 0.05.

(H) Current amplitude evoked by a −120-mV step in naive and unpaired-trained groups was significantly greater than that recorded in FC animals (one-way ANOVA: $F_{2,16} = 15.2$, $p < 0.0000001$). Tukey's post hoc: **p = 0.01, ***p < 0.001. (See Figure S3.)

(I and J) I_h recorded in stellate cells in lobule IX. (I) I_h amplitude in response to a −120-mV step recorded in lobule IX of naive (left panel) and FC (right panel) animals.

(J) Current-voltage relationship showing I_h amplitude was not significantly different between FC and naive animals in lobule IX (n = 5; two-way RM ANOVA: $F_{1,56} = 1.1$, $p = 0.32$). Data are represented as mean ± SEM.

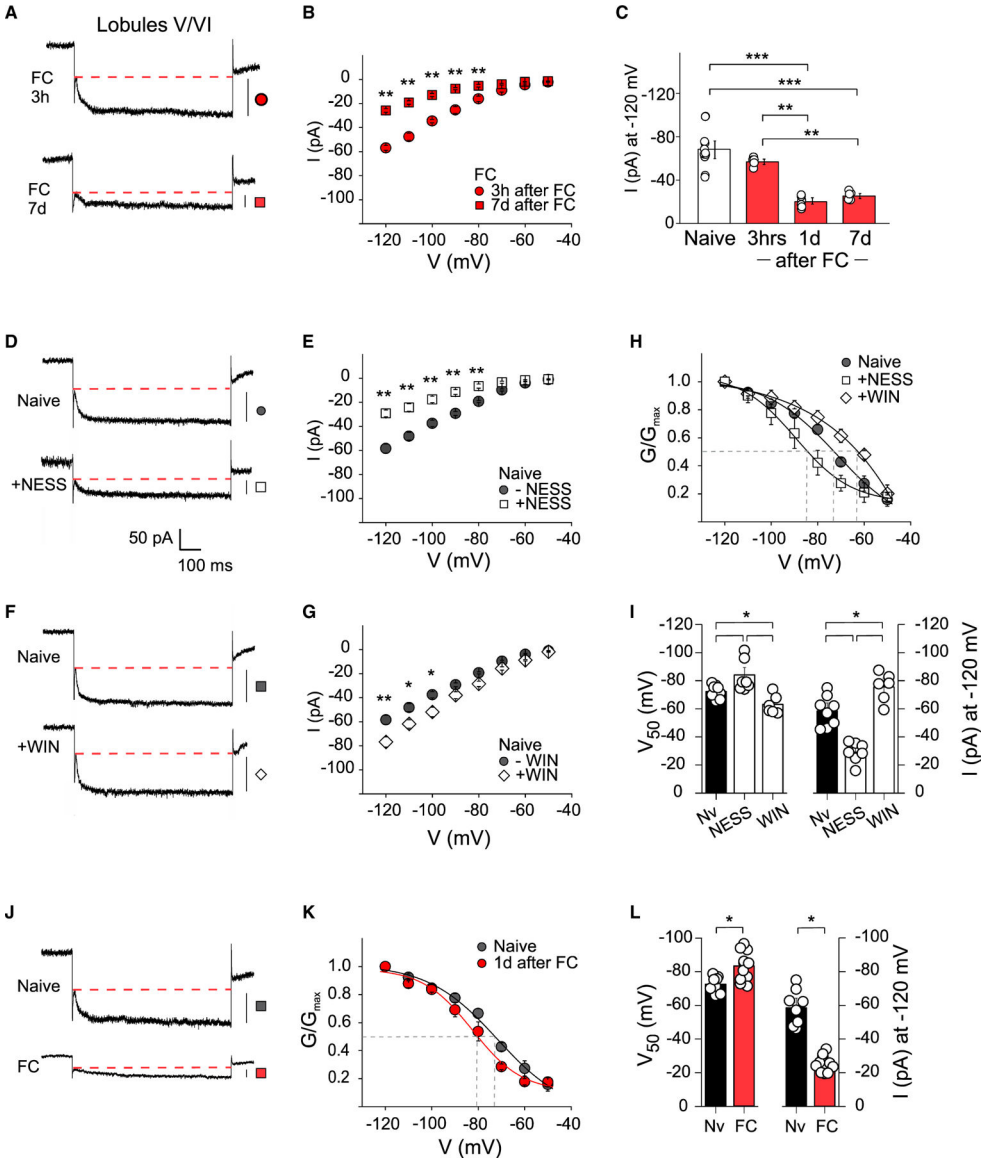

Figure 2. CB1Rs and fear conditioning modulate the amplitude and activation of I_h in stellate cells

(A–C) Time course of I_h recordings in SCs from lobules V/VI. (A) I_h amplitude in response to a −120-mV step recorded in 3 h (top panel) and 7 days post FC (bottom panel) animals. (B) Current-voltage relationship showing a decrease in I_h amplitude 7 days after FC (two-way RM ANOVA: $F_{7,63} = 65.02$, $p < 0.0001$). (C) Current amplitude evoked by a −120-mV step in SCs from 1 day and 7 days following FC groups was significantly lower than that recorded in naive and 3-h post-CF animals (one-way ANOVA: $F_{3,25} = 31.9$, $p < 0.0000001$). (B and C) Tukey's post hoc: **$p < 0.0001$, ***$p < 0.000001$. (See Figure S4.).

(D–I) Endocannabinoid signaling regulated I_h in stellate cells from naive mice.

(D) Representative traces of I_h recorded before and 10 min after bath application of NESS0327 (0.5 μM), a CB1R antagonist.

(E) Current-voltage relationship of I_h showing that NESS0327 reduced I_h amplitude (two-way RM ANOVA: $F_{7,91} = 22.06$, $p < 0.0001$).

(F and G) Application of the CB1R agonist, WIN55 212–2 (5 μM), increased I_h amplitude (two-way RM ANOVA: $F_{7,84} = 3.89$, $p = 0.001$; naive, same as E).
(H) HCN conductance (G)-voltage plots were fitted by a Boltzmann equation to obtain half-activation potential values (V_{50}, vertical dashed lines). NESS0327 and WIN55 212–2 caused a hyperpolarizing and depolarizing shift in the voltage-dependence of I_h activation, respectively (two-way RM ANOVA: $F_{12,108} = 2.98$, $p = 0.0013$).
(I) CB1R agonist and antagonist modified the amplitude and activation voltage of I_h (one-way ANOVA, V_{50}: $F_{2,18} = 10.4$, $p = 0.001$; I_h amplitude: $F_{2,18} = 39.4$, $p < 0.0001$).
(J–L) Fear conditioning reduced I_h amplitude and shifted I_h activation to a more hyperpolarized potential (n = 9), compared to naive control (same as I, n = 7; unpaired t test, V_{50}: $t_{15} = -9.1$, $p < 0.00001$; I_h amplitude: $t_{15} = -3.2$, $p = 0.005$).
(E, G, I, L) Tukey's post hoc: *p < 0.05, **p < 0.01. NESS: NESS0327; WIN: WIN55 212–2.
Data are represented as mean ± SEM.

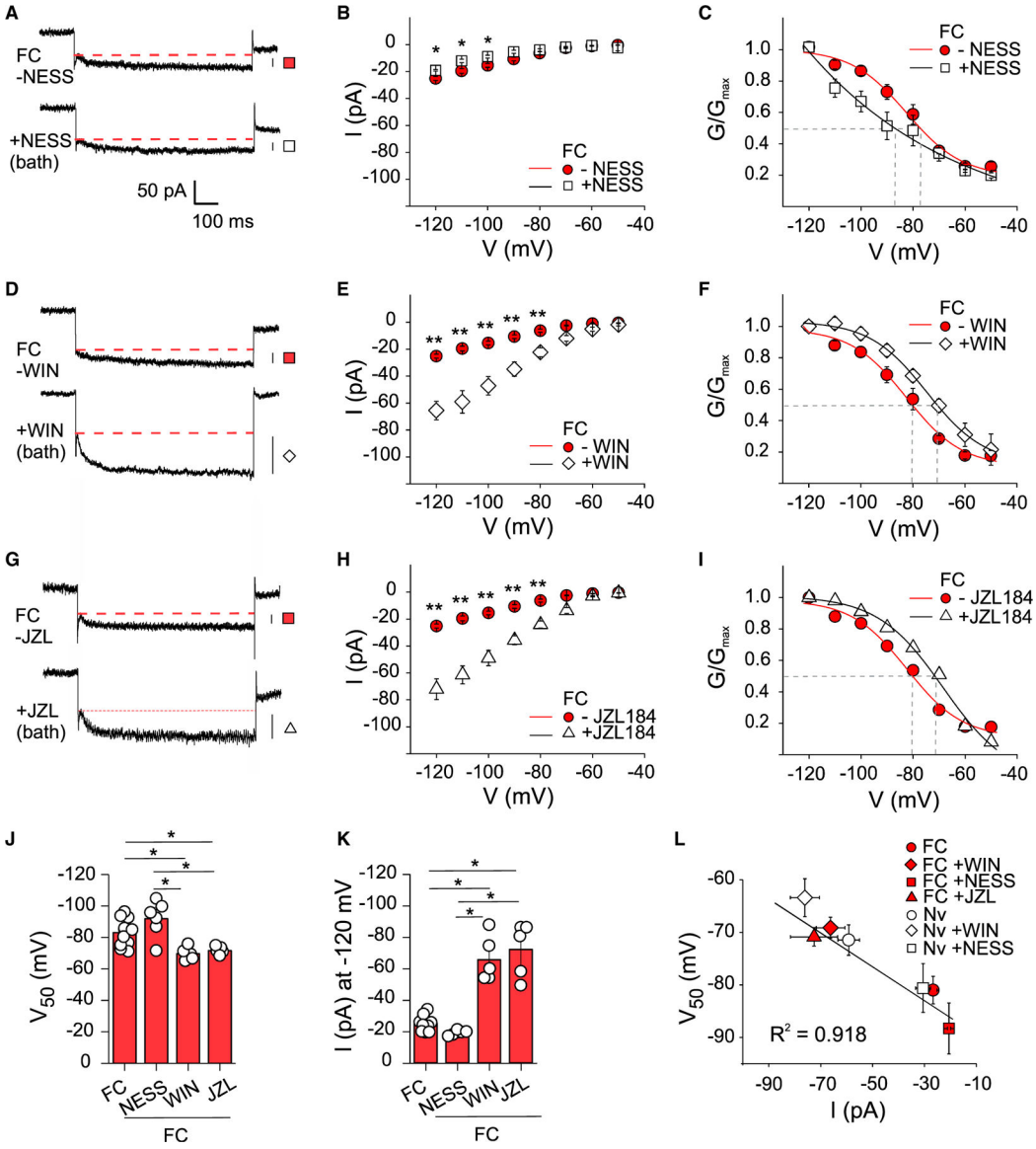

Figure 3. Fear conditioning decreases I_h by reducing endocannabinoid signaling

HCN channel currents recorded in SCs of lobules V/VI from conditioned animals prior to and during application of a CB1R antagonist (A–C), CB1R agonist (D–F), and MAGL antagonist (G–I). The CB1R antagonist, NESS0327, failed to alter I_h (A–C).

(A) Representative traces of I_h before and during NESS0327 application.

(B) Current-voltage relationship (n = 6; two-way RM ANOVA: $F_{7,105} = 6.68$, $p < 0.00001$).

(C) Voltage dependence of I_h activation (two-way RM ANOVA: $F_{6,90} = 1.71$, $p = 0.13$).

(D–F) I_h recorded before and during WIN55–212-2 application. WIN55–212-2 enhanced I_h and caused a depolarizing shift in I_h activation, reversing learning-induced changes (n = 5; two-way RM ANOVA: in E, $F_{7,98} = 47.99$, $p < 0.00001$; in F, $F_{6,84} = 1.22$, $p = 0.30$).

(G–I) I_h recorded before and during bath application of JZL184, a MAGL inhibitor, to increase endogenous 2-AG. This treatment led to an increase in I_h amplitude (n = 5;

two-way RM ANOVA: $F_{7,98} = 59.47$, $p < 0.0001$) and depolarizing shift in I_h activation (two-way RM ANOVA: $F_{6,84} = 4.79$, $p < 0.0003$).

(J and K) Fear conditioning occluded the NESS-induced decrease in I_h amplitude at −120 mV and hyperpolarizing shift in I_h activation observed in naive animals. The decrease in I_h was rescued by WIN55–212-2 and JZL184 (one-way ANOVA: V_{50}, $F_{3,23} = 9.3$, $p < 0.0003$; I_h, $F_{3,23} = 43.6$, $p = 0.0001$).

(L) A strong linear correlation was observed between the V_{50} value and the current amplitude in cells from both naive and FC mice ($R^2 = 0.92$). FC data in (C), (F), and (I) is the same as that in Figure 2K; (E) and (H) as in Figure 3B; and (J) and (K) as in Figure 2L.

Data are represented as mean ± SEM.

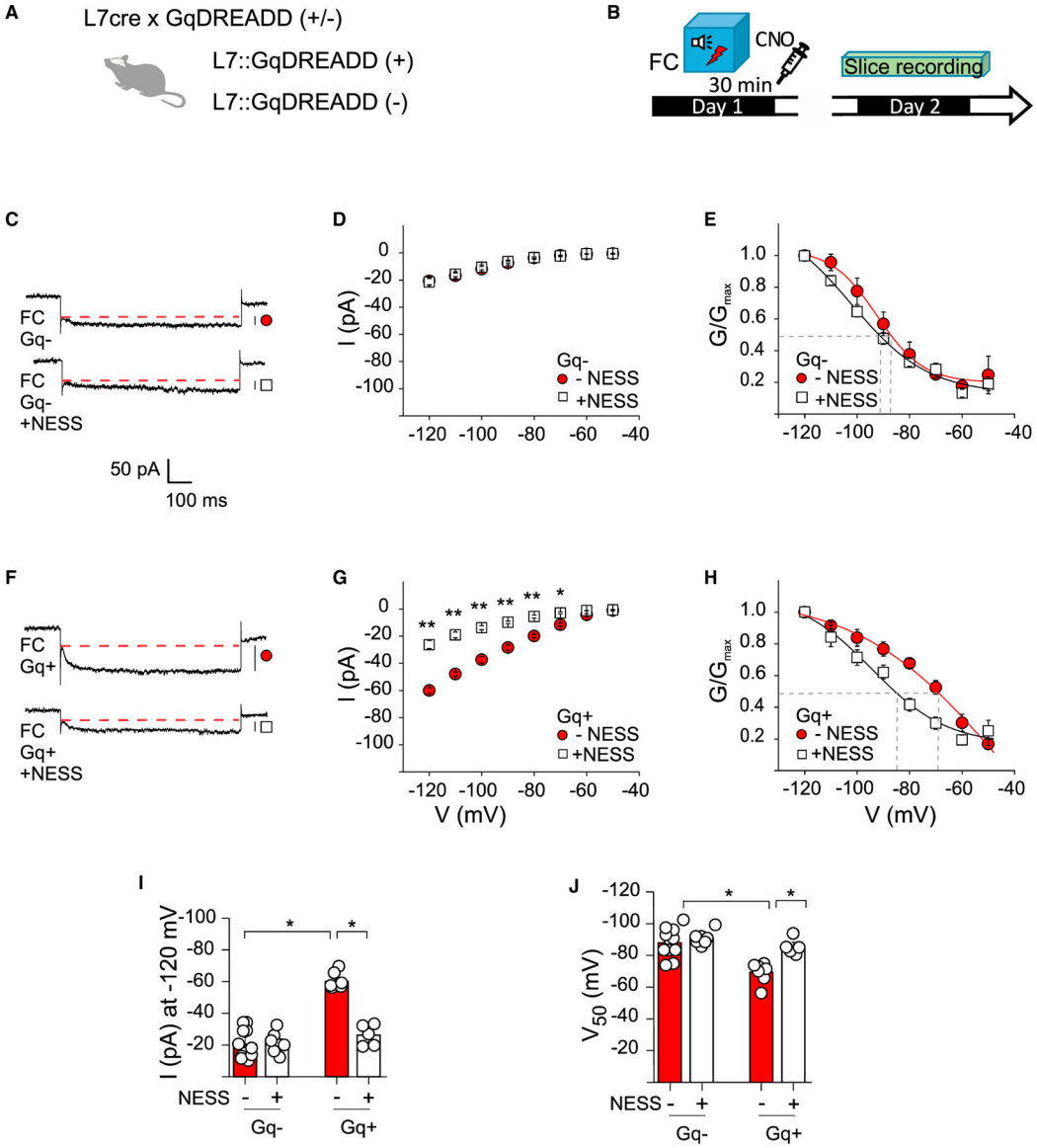

Figure 4. Endocannabinoids released *in vivo* prevent the learning-induced decrease in I_h

Activation of Gq-DREADD in PCs can trigger endocannabinoid release and disrupt memory consolidation. [10] This paradigm prevented the loss of SC I_h in lobules V/VI.

(A and B) Experimental protocol.

(C–E) I_h amplitude and activation voltage in SCs from L7:Gq(−) mice (n = 11) were comparable to those in conditioned wild-type (WT) mice and were not altered by CB1R antagonist (n = 7; two-way RM ANOVA: in D, $F_{7,112} = 0.21$, $p = 0.98$; in E, $F_{6,96} = 0.31$, $p = 0.93$).

(F–H) The amplitude and activation of SC I_h in L7:Gq(+) animals (n = 7) were indistinguishable from naive WT mice. Application of a CB1R antagonist reduced I_h amplitude and caused a hyperpolarization shift in activation voltage (n = 5; two-way RM ANOVA: in G, $F_{7,70} = 46.61$, $p < 0.0001$; in H, $F_{6,60} = 3.54$, $p = 0.0045$). (I and J) HCN channels in SCs from L7:Gq(+) mice exhibited greater I_h amplitude and were activated at

more depolarization potentials than L7:Gq(−) animals. These differences were lost in the presence of a CB1R antagonist (two-way RM ANOVA, I_h amplitude: $F_{1,26} = 34.0$, $p = 0.0001$; V_{50}: $F_{1,26} = 11.8$, $p = 0.002$). **$p < 0.001$, ***$p < 0.0001$.
Data are represented as mean ± SEM.

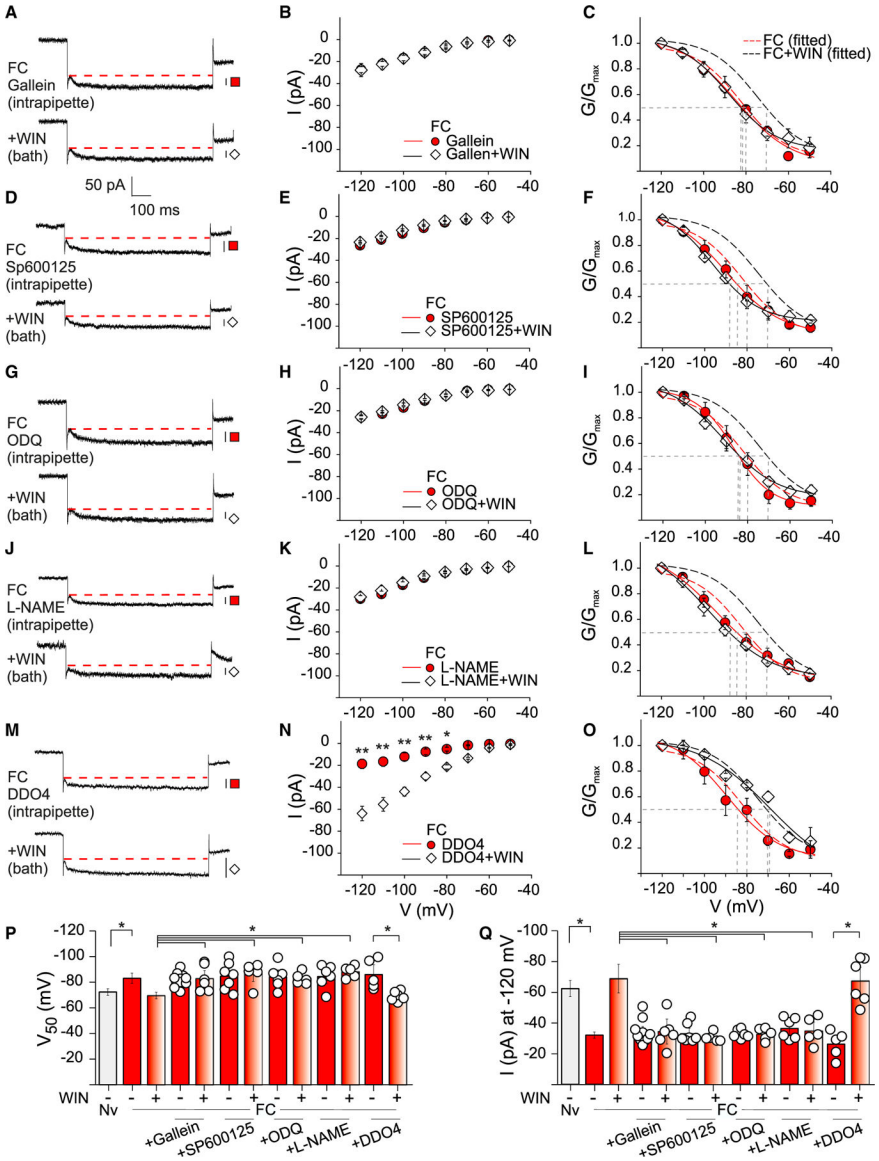

Figure 5. CB1R activation increases I_h via a $G_{\beta\gamma}$-JNK-NOS-cGMP-dependent pathway in stellate cells

Effects of $G_{\beta\gamma}$-JNK-NOS-cGMP pathway inhibition on I_h in cerebellar SCs from conditioned mice prior to and during bath application of WIN55 212–2.

(A) Representative traces of I_h in the presence of the $G_{\beta\gamma}$ inhibitor, gallein (10 μM).

(B and C) Intracellular application of gallein did not alter the amplitude or activation of I_h after FC but prevented the WIN-induced increase in these measures (n = 6).

(D–L) Antagonists of JNK (10 μM SP600125; n = 5; D–F), GC (10 μM ODQ; n = 5; G–I), and NOS (100 μM L-NAME, n = 5; J–L) also blocked WIN-induced changes in current amplitude and activation voltage without affecting basal I_h.

(M–O) Intracellular application of an AC inhibitor (15 μM DDO4, n = 6) failed to prevent WIN-induced changes in I_h amplitude and activation voltage (two-way RM ANOVA: in N, $F_{7,63} = 22.32$, $p < 0.0001$; in O, $F_{6,30} = 1.90$, $p = 0.04$).

(P and Q) $G_{\beta\gamma}$, GC, NOS, and JNK inhibitors all prevented the CB1R-dependent increase in I_h amplitude and depolarizing shift in activation (two-way ANOVA, I_h: $F_{5,65} = 17.91$, $p < 0.0001$; V_{50}: $F_{5,65} = 3.52$, $p = 0.007$). These findings indicate that CB1R activates a $G_{\beta\gamma}$-JNK-NOS-GC pathway to elevate cGMP levels and increase the amplitude of I_h. Data are represented as mean ± SEM; *$p < 0.05$, **$p < 0.01$.

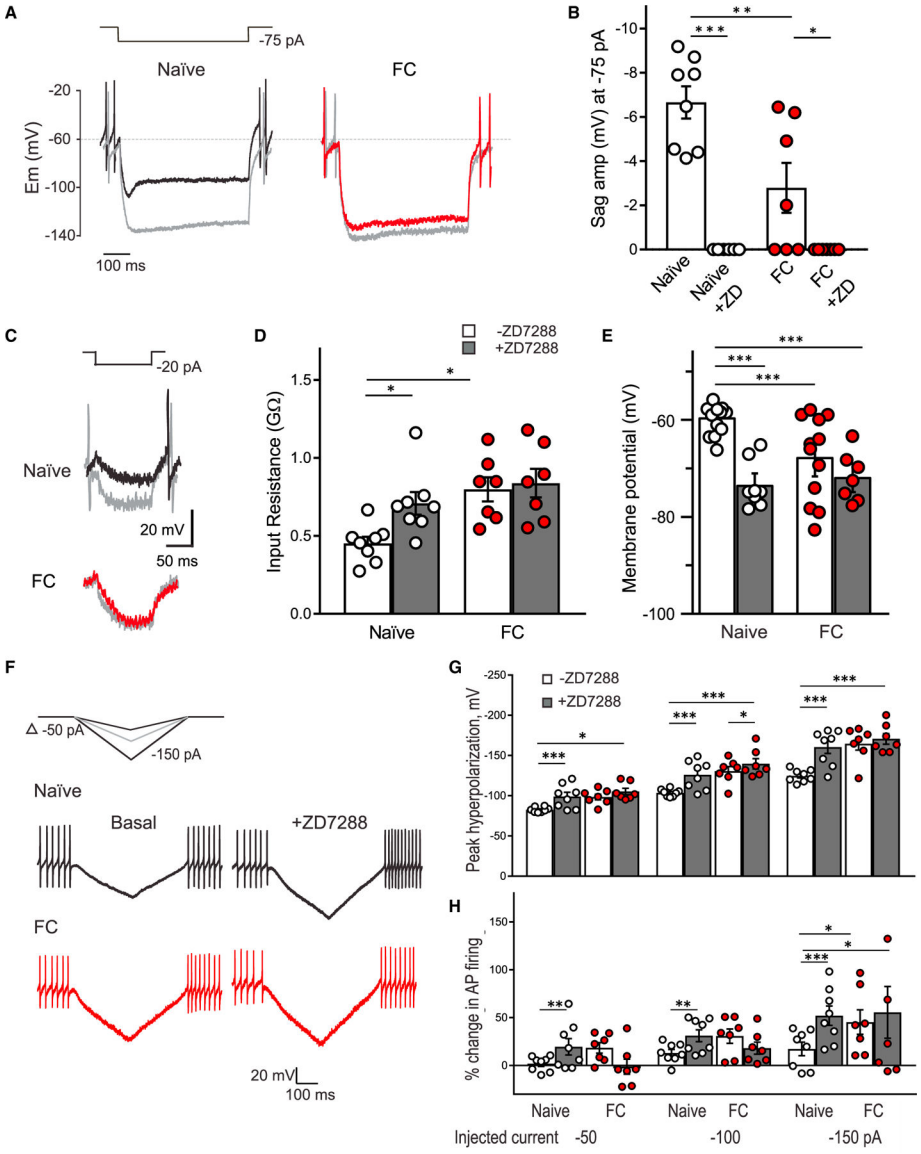

Figure 6. Reduction of I_h alters intrinsic membrane properties and augments the stellate cell response to hyperpolarizing input

(A) Injection of a negative current step (−75 pA) produced a rapid hyperpolarization followed by a depolarizing inflection in naive cells (n = 8; black trace), which was completely blocked by application of ZD7288 (gray trace). The sag response was markedly reduced in recordings from FC animals (n = 7; red trace).

(B) Quantification of the change in voltage sag revealed a reduction in cells from FC animals that was consistent with a decrease in functional HCN (two-way RM ANOVA: $F_{1,13} = 8.7$, $p = 0.011$).

(C) Voltage responses to a −20-pA current injection in both naive and learned-fear groups.

(D) FC increased SC input resistance relative to naive animals (two-way RM ANOVA: $F_{1,13} = 8.06$, $p = 0.014$).

(E) Cells from naive animals (n = 8) exhibited a more depolarized membrane potential than those from FC animals (n = 7; unpaired t test: p = 0.034). The difference was lost in the presence of ZD7288 (two-way ANOVA, $F_{1,35} = 6.1$, p = 0.018).
(F and G) Sample traces of the SC response to a −100-pA bidirectional current ramp. Summary data of peak hyperpolarization revealing greater voltage deflections in SCs from naive animals after I_h blockade and from FC vs. naive mice (two-way RM ANOVA: $F_{1,13} = 25.3$, p = 0.0002).
(H) Blockade of I_h in cells from naive animals increased the instantaneous firing observed on relief of injected currents (calculated as percent change in frequency). Injection of −150 pA resulted in a greater change in action potential firing in FC vs. naive animals. Holm-Sidak post hoc: *p < 0.05, ***p % 0.0001.
Data are represented as mean ± SEM.

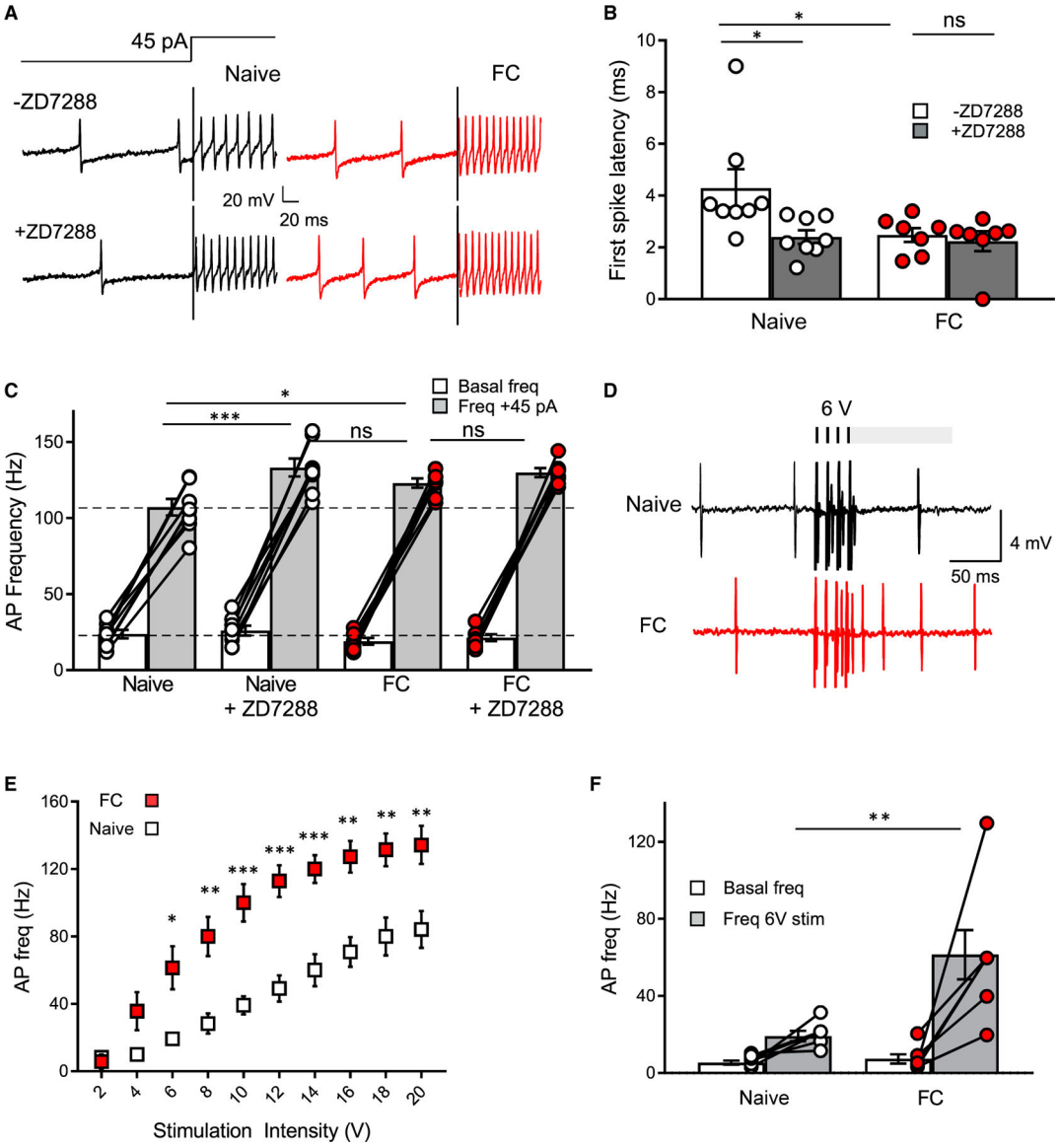

Figure 7. Learning-induced reductions in I_h increase the input-output relationship of cerebellar stellate cells and enhance the response to parallel fiber stimulation

(A) Traces from naive and FC animals showing SC spike output in response to a 45-pA depolarizing current step.

(B) Inhibition of I_h through application of ZD7288 markedly reduced the first-spike latency (two-way RM ANOVA: $F_{1,13} = 4.97$, $p = 0.044$; Holm-Sidak post hoc test: *$p = 0.008$), and the depletion in stellate cell I_h following learning shortened the first-spike latency ($p = 0.014$).

(C) I_h blockade enhanced action potential frequency in response to a 45-pA current injection (Tukey's test, $p < 0.0001$). Moreover, the frequency response of FC cells was higher when compared to that of naive cells ($p = 0.028$)—a difference that was lost when compared to naive cells after application of ZD7288 ($p = 0.25$).

(D) Traces from naive and FC animals showing action potentials elicited in response to 6-V parallel fiber stimulations.

(E) Fear learning lowered the threshold at which cells responded to parallel fiber stimulation (two-way RM ANOVA: $F_{9,99} = 5.3$, $p < 0.0001$).
(F) At the 6-V stimulation intensity, the firing rate of the FC group was 2-fold greater than that of the naive group (Holm-Sidak: $p = 0.0008$), while no difference was observed in basal firing between conditions ($p = 0.98$). *p < 0.05, **p < 0.001, ***p % 0.0001.
Data are represented as mean ± SEM.

KEY RESOURCES TABLE

REAGENT or RESOURCE	SOURCE	IDENTIFIER
Bacterial and virus strains		
(AAV) pAAV-hSyn-DIO-hM4D(Gi)-mCherry	Chan et al.[57]	RRID: Addgene Plasmid #44362
AAV-hSyn-DIO-mCherry	Bryan Roth	RRID: Addgene Plasmid #50459
Chemicals, peptides, and recombinant proteins		
clozapine N-oxide (CNO)	Cayman Chemical Company	Item#25780
ZD7288 (ab120102)	Abcam Biochemicals	Ab120102
WIN55,212–2	Ascent-Scientific	Asc-085
NESS0327	Cayman Chemical Company	Item#10004184
JZL184	Enzo life sciences	BML-EI391
Gallein	Hello bio	HB3050
SP600125	Hello bio	HB2234
ODQ	Tocris	Cat#0880
L-NAME	Hello bio	HB1352
2′, 5′ -Dideoxy Adenosine (DDO4)	Cayman Chemical Company	Item#20358
Picrotoxin	Indofine Chemical Company	Cat#P-001
SR 95531	Abcam Biochemicals	ab120042
TTX	Ascent-Scientific	Asc-054
Kynurenic acid	Tocris	Cat#0223
Experimental models: Organisms/strains		
C57Bl/6J wild-type	Jackson Laboratory	RRID:IMSR_JAX:000664
NOS::CRE (B6.129-Nos1/J)	Jackson Laboratory	RRID:IMSR_JAX:017526
B6N; 129-Tg(CAG-CHRM3*,-mCitrine) 1Ute/J	Jackson Laboratory	RRID:IMSR_JAX:026220
B6.129-Tg(Pcp2-cre)2Mpin/J	Jackson Laboratory	RRID:IMSR_JAX:004146